The contributions of host population size and maternal transmission rate to fluctuating *Wolbachia* frequencies

Jason M. Graham[1], Joseph Klobusicky[1], Michael T.J. Hague[2,*]

[1]Mathematics Department
University of Scranton
Scranton, PA 18510

[2]Biology Department
University of Scranton
Scranton, PA 18510

[*]**Corresponding Author**
Michael T.J. Hague
Biology Department
University of Scranton
800 Linden Street
Scranton, PA 18510
(570) 941-7962
michael.hague@scranton.edu

Keywords: host-microbe interaction, endosymbiosis, vertical transmission, *w*Mel, *Wolbachia*, *Drosophila*

Running Head: Fluctuating *Wolbachia* frequencies

ABSTRACT

Many insects and other animals host maternally transmitted endosymbionts that alter host fitness and reproduction. The facultative endosymbiont *Wolbachia* is found in roughly half of all insect species, but population frequencies fluctuate across time and geography for unknown reasons. This is especially true for *w*Mel *Wolbachia* in *Drosophila melanogaster* and related "*w*Mel-like" strains that fluctuate over timescales as short as a month. Recent work suggests these fluctuations may be due to temperature effects that disrupt maternal transmission in some or all female hosts under certain conditions. We simulated temporal *Wolbachia* dynamics in the new R package *wlbcmodeler* to test whether fluctuations can be solely explained by finite-host population stochasticity or, alternatively, by perturbation of maternal transmission rates. Across a range of biologically plausible parameters, we show that declining transmission rates increase variance and decrease mean *Wolbachia* frequencies over time, and these effects outweigh the impact of *Wolbachia* effects on host fitness (i.e., fecundity) and *Wolbachia*-induced cytoplasmic incompatibility. Large temporal fluctuations can arise due to stochasticity or changes to maternal transmission rates that alter *Wolbachia* equilibria. These simulated dynamics may explain fluctuations of *w*Mel-like *Wolbachia* over years-long periods, but additional factors (e.g., insect demography) likely contribute to fluctuations over shorter timescales.

INTRODUCTION

Animal life is characterized by interactions with microbes that span a continuum from beneficial to antagonistic. Many insects and other animals carry heritable endosymbionts that reside within their own cells. These microorganisms can alter basic aspects of host fitness, including reproduction, immune function, and nutrient acquisition (McFall-Ngai et al. 2013; Shropshire et al. 2020; Perreau and Moran 2022; Bennett et al. 2024; Hoffmann and Cooper 2024). Heritable endosymbionts often form close associations with female ovaries and the germline to ensure that microbes are maternally transmitted from one host generation to the next (Russell et al. 2019; Hague et al. 2024). This process of vertical-maternal transmission is a key determinant of the spread, persistence, and long-term evolutionary dynamics of endosymbiosis. Strict vertical maternal transmission aligns the fitness interests of both hosts and endosymbionts, which may lead to long-term, stable relationships that can approach the status of organelles (Wade 2007; McCutcheon and Moran 2012; Fisher et al. 2017; McCutcheon et al. 2019; Perreau and Moran 2022).

Ultimately, the ecological and evolutionary consequences of endosymbioses are determined by whether or not endosymbionts are prevalent in host populations. Many endosymbionts are facultative from the host perspective, such that a proportion of host individuals in the population do not carry endosymbionts due to imperfect maternal transmission (Mateos et al. 2006; Carrington et al. 2011; Hamm et al. 2014; Corbin et al. 2017; Hague et al. 2020*b*). The frequency of facultative endosymbionts in host populations can vary widely across host systems, geography, and time (Hamm et al. 2014; Kriesner et al. 2016; Cooper et al. 2017; Hague et al. 2020*b*), suggesting that variable maternal transmission rates contribute to variation in endosymbiont prevalence. For instance, if maternal transmission is perturbed by

environmental conditions (e.g., temperature), high rates of imperfect maternal transmission may cause endosymbiont frequencies to decline in certain host populations (Hague et al. 2020*b*, 2022; Ross et al. 2020). Nonetheless, the relative contribution of imperfect maternal transmission to variation in endosymbiont prevalence is poorly understood, especially in the context of other important contributing factors, such as endosymbiont effects on host fitness and stochastic dynamics associated with host population size (Caspari and Watson 1959; Hoffmann et al. 1990).

Maternally transmitted *Wolbachia* are the most common endosymbionts on earth, infecting roughly half of all insect species, as well as other arthropods and nematodes (Ferri et al. 2011; Zug and Hammerstein 2012; Weinert et al. 2015). *Wolbachia* are vertically-maternally transmitted through the female germline (Russell et al. 2019; Porter and Sullivan 2023; Radousky et al. 2023; Hague et al. 2024); although, phylogenetic evidence indicates that horizontal and introgressive transfers occur frequently on evolutionary timescales (O'Neill et al. 1992; Raychoudhury et al. 2009; Conner et al. 2017; Gerth and Bleidorn 2017; Turelli et al. 2018; Cooper et al. 2019; Vancaester and Blaxter 2023; Shropshire et al. 2024). *Wolbachia* generally form facultative relationships with insects (from the host perspective), as the endosymbionts are usually found in only a proportion of host individuals due to imperfect maternal transmission. *Wolbachia* frequencies have been shown to vary considerably among and within host systems (Hoffmann et al. 1990; Kriesner et al. 2013, 2016; Hamm et al. 2014; Cooper et al. 2017; Hague et al. 2020*b*, 2022; Turelli et al. 2022); however, the relative contribution of imperfect maternal transmission to this frequency variation is unclear.

Population frequencies and equilibria dynamics of *Wolbachia* can be approximated by a discrete generation, deterministic model that incorporates three parameters: (1) the proportion of

uninfected ova produced by *Wolbachia*-positive females (μ; i.e., imperfect maternal transmission), (2) the fitness of *Wolbachia*-positive females relative to *Wolbachia*-negative females (F; i.e., components of host fitness like fecundity), and (3) the relative egg hatch of uninfected eggs fertilized by *Wolbachia*-positive males (s_h) due to *Wolbachia*-induced cytoplasmic incompatibility (CI) (Hoffmann et al. 1990). The initial spread and persistence of *Wolbachia* in natural host populations is generally considered to be driven by beneficial effects on host fitness ($F > 1$), which are balanced by imperfect maternal transmission ($\mu > 0$) (Hoffmann et al. 1990; Turelli and Hoffmann 1991; Kriesner et al. 2013; Kriesner and Hoffmann 2018; Ross et al. 2019*b*; Turelli et al. 2022). Although beneficial *Wolbachia* effects on host fitness are poorly understood in nature, recent work suggests *Wolbachia* block viruses in their native *Drosophila* hosts (Hedges et al. 2008; Teixeira et al. 2008; Osborne et al. 2009; Martinez et al. 2014; Cogni et al. 2021; Bruner-Montero and Jiggins 2023), in addition to a potential role of nutrient provisioning (Brownlie et al. 2009; Nikoh et al. 2014; Newton and Rice 2020). Some *Wolbachia* strains also cause CI ($s_h > 0$), a crossing incompatibility that generates a frequency dependent benefit for *Wolbachia*-positive females (Shropshire et al. 2020; Turelli et al. 2022). Once a CI-causing strain exceeds a critical frequency threshold, *Wolbachia* will rapidly spread to high frequencies, which are balanced by imperfect maternal transmission (Hoffmann and Turelli 1988; Hoffmann et al. 1990; Turelli and Hoffmann 1995; Carrington et al. 2011; Kriesner et al. 2013; Turelli et al. 2022).

In host systems where *Wolbachia* do not cause strong CI, infection frequencies tend to fluctuate across time and geographic space (Kriesner et al. 2013, 2016; Hamm et al. 2014; Cooper et al. 2017; Hague et al. 2020*b*). For instance, *w*Mel in *Drosophila melanogaster* and the closely related ("*w*Mel-like") *w*San and *w*Yak strains in *D. yakuba*-clade hosts (diverged from

89 *w*Mel ~30,000 years ago) generally cause no or weak CI. The frequencies of these *w*Mel-like
90 *Wolbachia* can fluctuate dramatically over time periods as short as a month at a given location
91 (Figure 1) (Hoffmann et al. 1998; Reynolds and Hoffmann 2002; Cooper et al. 2017, 2019). For
92 example, at Gold Coast in subtropical eastern Australia, the frequency (p) of *w*Mel in *D.*
93 *melanogaster* dropped from $p = 0.919$ (binomial confidence interval: 0.787, 0.972) in March
94 1995 down to $p = 0.25$ (0.12, 0.449) just a month later in April and then rebounded back up to p
95 $= 0.615$ (0.355, 0.823) in September (Hoffmann et al. 1998). Similarly, on the island of São
96 Tomé off the coast of west Africa, the frequency of *w*San in host *D. santomea* dropped from $p =$
97 0.772 (0.648, 0.862) in 2009 to $p = 0.368$ (0.234, 0.527) in 2015 and then back up to $p = 0.795$
98 (0.692, 0.87) in 2018 (Cooper et al. 2017; Hague et al. 2020*b*). The frequencies of *w*Mel and *D.*
99 *yakuba*-clade *Wolbachia* have also been shown to vary geographically among host populations
100 by latitude and altitude (Kriesner et al. 2016; Cooper et al. 2017; Hague et al. 2020*b*). These
101 variable patterns contrast those of strong CI-causing *Wolbachia* strains (e.g., *w*Ri in *D.*
102 *simulans*), which tend to persist at high, stable frequencies due to the frequency dependent
103 advantage of CI (Hoffmann et al. 1990; Turelli and Hoffmann 1991, 1995; Rousset and Solignac
104 1995; Bourtzis et al. 1996; James and Ballard 2000; Ballard 2004; Carrington et al. 2011; Choi et
105 al. 2015; Turelli et al. 2018).

106 The temporal fluctuations of *w*Mel-like *Wolbachia* could be strictly due to stochasticity
107 associated with a finite host population. Alternatively, changes in the maternal transmission rate,
108 host fitness effects, and/or CI between host generations could generate deterministic changes to
109 *Wolbachia* equilibria over time. We first explore the hypothesis that *Wolbachia* frequencies
110 fluctuate over time as a result of finite-population stochasticity (Jansen et al. 2008; Kriesner and
111 Hoffmann 2018; Turelli and Barton 2022; Turelli et al. 2022). The deterministic model of

112 *Wolbachia* equilibria can be adapted to approximate the stochasticity induced by finite
113 population size using a stochastic transition matrix analogous to a haploid Wright-Fisher model
114 of genetic drift (Crow and Kimura 1970; Turelli and Barton 2022; Turelli et al. 2022). The model
115 uses an effective population size of N female hosts (because *Wolbachia* are maternally
116 transmitted) and binomial sampling to model the stochastic effect of finite population size and
117 their interactions with maternal transmission (μ), host fitness effects (F), and CI (s_h). Following
118 Turelli et al. (2022) and Turelli and Barton (2022), we evaluate how host population size
119 influences the stochasticity of *Wolbachia* frequencies over time, measured as the standard
120 deviation of *Wolbachia* frequencies (p_{SD}), in simulated host populations across a wide range of
121 biologically plausible values for *w*Mel-like *Wolbachia*. We also explored how different values of
122 μ, in conjunction with F and s_h, impact the magnitude of stochastic fluctuations over time.
123 Second, we investigate the hypothesis that *Wolbachia* frequencies may change
124 deterministically over time as a result of temporal changes in the maternal transmission rate, host
125 fitness effects, or CI strength between host generations (Turelli and Hoffmann 1995; Carrington
126 et al. 2011; Hague et al. 2020*b*). Recent work on *w*Mel and *w*Yak showed that rearing hosts at a
127 relatively cool temperature (20ºC) reduces maternal transmission rates compared to standard
128 conditions (25ºC) (Hague et al. 2020*b*, 2022). Maternal transmission estimates from field-
129 collected females in these systems also indicate that a proportion of *Wolbachia*-positive females
130 may be "low transmitters" with especially high rates of imperfect maternal transmission ($\mu > 0.7$)
131 (Hoffmann et al. 1998; Carrington et al. 2011; Hamm et al. 2014; Hague et al. 2020*b*). This
132 phenomenon has been observed in wild-caught females transmitting *w*Mel (Hoffmann et al.
133 1998), *w*San, and *w*Yak (Hague et al. 2020*b*), as well as other *Wolbachia* strains (Carrington et
134 al. 2011; Hamm et al. 2014). Thus, it is conceivable that rapid changes in environmental

conditions (e.g., a bout of cold weather) could perturb maternal transmission for all hosts or a subpopulation of low transmitters, causing deterministic changes to *Wolbachia* frequencies in subsequent host generations. Changes in the strength of host fitness effects or CI could similarly generate deterministic *Wolbachia* fluctuations, because these factors can also be context-dependent, for example, depending on environmental conditions, host age, and the *Wolbachia* and host genomes (Hoffmann et al. 1990; Clancy and Hoffmann 1998; Olsen et al. 2001; Reynolds and Hoffmann 2002; Bordenstein and Bordenstein 2011; Versace et al. 2014; Kriesner et al. 2016; Cooper et al. 2017; Cao et al. 2019; Shropshire et al. 2021). We used the stochastic model to evaluate how biologically plausible values of μ, F, and s_h influence *Wolbachia* equilibria, measured as the mean *Wolbachia* frequency ($\bar{p}$) from each simulated host population.

We implemented the simulations in the new publicly available R package *wlbcmodeler*. The package simulates temporal *Wolbachia* dynamics within a host population with discrete generations and a given effective population size. We used the R package to run 491,400 simulations across 3,276 unique parameter combinations to explore how biologically plausible values of host population size ($10^3 \leq N \leq 10^6$), imperfect maternal transmission ($0.001 \leq \mu \leq 0.5$), host fitness effects ($1 \leq F \leq 1.5$), and CI ($s_h = 0$ or 0.1) influence the temporal dynamics of *w*Mel-like *Wolbachia*. The package treats μ as a random binomial variable and allows for the inclusion of a subpopulation of low transmitter females (e.g., 10% of *Wolbachia*-positive females with $\mu = 0.8$). We also allow for fluctuating host fitness effects by treating F as a log-normal random variable (Turelli et al. 2022). We began each simulation at an arbitrary intermediate *Wolbachia* frequency of $p_0 = 0.4$ and ran the population for 10,000 host generations. After removing the initial 500 host generations as burn-in, we calculated the standard deviation (p_{SD}) and mean ($\bar{p}$) *Wolbachia* frequency from generations 501-10,000 for each simulation.

158 Broadly, our results demonstrate that strains that cause weak or no CI, such as *w*Mel-like
159 *Wolbachia*, tend to generate larger stochastic fluctuations over time compared to strong-CI
160 causing strains like *w*Ri in *D. simulans*. While the simulated stochastic and/or deterministic
161 dynamics in our model may explain the observed fluctuations of *w*San on São Tomé over years-
162 long periods, other factors likely contribute to the fluctuations of *w*Mel at Gold Coast over much
163 shorter month-long periods.
164

165 **THEORETICAL FRAMEWORK**

166 *Deterministic analysis of Wolbachia frequencies*

167 The deterministic model of *Wolbachia* population frequencies and equilibria dynamics
168 incorporates imperfect maternal transmission (μ), host fitness effects modeled as differential
169 fecundity (F), and CI (s_h) (Hoffmann et al. 1990). We assume that uninfected ova produced by
170 *Wolbachia*-positive females (due to imperfect maternal transmission) are susceptible to CI, just
171 as uninfected ova from *Wolbachia*-negative females (Carrington et al. 2011). Embryos produced
172 by fertilizations of *Wolbachia*-negative ova with sperm from *Wolbachia*-positive males hatch
173 with frequency $H = 1 - s_h$ relative to the other three possible fertilizations, which are all
174 considered equally compatible (Cooper et al. 2017). Thus, s_h represents the severity of CI, or the
175 frequency of unhatched eggs in pairings between *Wolbachia*-negative ova and *Wolbachia*-
176 positive sperm.

177 We first ignore CI and consider a stable equilibrium ($\hat{p}$) balanced by positive host fitness
178 effects ($F > 1$) and imperfect maternal transmission ($\mu > 0$) (Figure 2). When initially rare,
179 *Wolbachia* must generate $F(1 - \mu) > 1$ to spread deterministically from low frequency, regardless
180 of whether they cause CI. Here, we assume $F(1 - \mu) > 1$ given the spread and persistence of non-

181 CI causing *Wolbachia* strains in nature (Hoffmann and Turelli 1997; Kriesner et al. 2013, 2016;
182 Hamm et al. 2014; Kriesner and Hoffmann 2018; Meany et al. 2019). In contrast, when $F(1-\mu)$
183 < 1, rare infections will be deterministically lost (Hoffmann et al. 1990). A value of $F(1-\mu) > 1$
184 also provides an explanation for the low frequency spread of strong CI-causing strains,
185 particularly *w*Ri (Turelli and Hoffmann 1991, 1995; Bakovic et al. 2018). When $F(1-\mu) > 1$, the
186 stable equilibrium frequency is

$$\hat{p} = 1 - \frac{\mu F}{F-1}. \quad [1]$$

187 In this case, $\hat{p}$ increases from 0 to $1-\mu$ as F increases from $1/(1-\mu)$.

188 We explored a range of plausible μ values based on previous estimates of maternal
189 transmission in the field, as well as under varying conditions in the lab. Empirical estimates of
190 mean μ values ($\pm BC_a$ confidence intervals) for *w*Mel generated from field-collected *D.*
191 *melanogaster* have ranged from low ($\mu = 0.026$ [0.008, 0.059]; Hoffmann et al. 1998) up to
192 moderate levels of imperfect transmission ($\mu = 0.11$ [0.07, 0.17]; Olsen et al. 2001). Estimates
193 generated in the lab range as high as $\mu = 0.415$ (0.332, 0.493) when females are reared in the
194 cold (20ºC) relative to a standard temperature (25ºC) (Hague et al. 2022, 2024). Estimates of
195 mean μ values for *w*San from field collected *D. santomea* on the island of São Tomé were
196 moderate ($\mu = 0.068$ [0.027, 0.154]), whereas *w*Yak in *D. yakuba* ranged from low at low
197 altitude ($\mu = 0.038$ [0.003, 0.184]) to moderate at high altitude ($\mu = 0.20$ [0.087, 0.364]) (Hague
198 et al. 2020*b*). Estimates of μ generated under lab conditions for *w*Yak in *D. yakuba* ranged as
199 high as $\mu = 0.15$ (0.109 0.196) when females were reared in the cold (Hague et al. 2020*b*). We
200 thus decided to explore a broad range of μ values from $0.001 \leq \mu \leq 0.5$.

201 We know far less about *Wolbachia* effects on host fitness (F) in natural populations due
202 to the challenges of estimating fitness of *Wolbachia*-positive and -negative individuals in the

203 wild (Ross et al. 2019*b*). *Wolbachia* cells are found throughout host somatic tissue (Pietri et al.
204 2016), which is likely to have complex effects on components of host fitness in nature
205 (Hoffmann et al. 1998; Weeks et al. 2007; Kriesner et al. 2016; Hague et al. 2020*a*, 2021; Cogni
206 et al. 2021; Bruner-Montero and Jiggins 2023). Prior work found no evidence for fecundity
207 effects of *w*Mel in *D. melanogaster* (Hoffmann et al. 1994) or *Wolbachia* in *D. yakuba*-clade
208 hosts (Cooper et al. 2017); however, fecundity represents only one aspect of host fitness.
209 *Wolbachia* effects on other measures of host fitness in the lab have ranged from negative
210 (Hoffmann and Turelli 1988; Hoffmann et al. 1990; Kriesner et al. 2016) to positive (Hedges et
211 al. 2008; Teixeira et al. 2008; Brownlie et al. 2009; Russell et al. 2023) to context-dependent
212 (Olsen et al. 2001; Fry et al. 2004). Beneficial *Wolbachia* effects of $F > \sim 1.2$ (roughly a 20%
213 relative fitness advantage for *Wolbachia*-positive females) have not been documented in any
214 system (Weeks et al. 2007; Hamm et al. 2014; Meany et al. 2019; Hague et al. 2020*b*). We
215 generally expect $F > 1$ based of the spread and persistence of *Wolbachia* strains in natural host
216 populations (described above); however, we expect values of $F > 1.5$ to be biologically
217 unrealistic (Weeks et al. 2007; Hamm et al. 2014; Cooper et al. 2017; Meany et al. 2019; Hague
218 et al. 2020*b*, 2022). Therefore, we chose to explore F values ranging from $1 \leq F \leq 1.5$.
219 Next, we considered equilibria that incorporate CI ($s_h > 0$) (Figure 2). Like non-CI
220 causing strains, CI-causing strains must still increase host fitness to spread deterministically from
221 low frequency such that $F(1 - \mu) > 1$. CI-causing infections that generate $F(1 - \mu) > 1$ and $F\mu <$
222 1 produce a single stable equilibrium between 0 and 1 given by

$$\hat{p} = \frac{s_h + 1 - F + \sqrt{(s_h + 1 - F)^2 + 4s_h[F(1-\mu) - 1](1 - F\mu)}}{2s_h(1 - F\mu)}. \quad [2]$$

223 Prior estimates of CI using field-collected *D. melanogaster* males from central and northern
224 Australia suggest that *w*Mel causes weak CI on the order of $s_h = 0.05$ (Hoffmann et al. 1998;

225 Kriesner et al. 2016). CI strength declines rapidly with male age (Shropshire et al. 2021) and
226 Reynolds and Hoffmann (2002) found that one-day-old males derived from wild-collected larvae
227 and pupae produce hatch rates of 0.39 in incompatible crosses, with large confidence intervals
228 (0.15, 0.64). Given this information, Kriesner et al. (2016) conjectured that s_h values for *w*Mel of
229 0 to 0.1 are plausible, but $s_h > 0.1$ is unlikely. We are not aware of CI estimates for *D. yakuba*-
230 clade *Wolbachia* using field-collected males; however, estimates in the laboratory indicate that
231 these strains reduce egg-to-adult viability in CI crosses by about 10-20% (*w*San: $s_h = 0.15$ [0.12,
232 0.18]; *w*Yak: $s_h = 0.16$ [0.13, 0.20]; *w*Tei: $s_h = 0.2$ [0.17, 0.23]), although the presence and
233 intensity of CI can also vary depending on host and *Wolbachia* genotype (Cooper et al. 2017).
234 Based on these previous data, we decided to explore the effects of weak CI ($s_h = 0.1$) on
235 *Wolbachia* equilibria and temporal dynamics. We also considered strong CI ($s_h = 0.45$) that is
236 characteristic of field-collected male *D. simulans* carrying *w*Ri (Turelli and Hoffmann 1995;
237 Carrington et al. 2011); although, this level of CI has not been observed for the *w*Mel-like
238 *Wolbachia* described here.

239 Assuming discrete host generations, the total population fraction of offspring in the next
240 generation can be divided with respect to whether mated males and females are carrying
241 *Wolbachia*:

242 1. *Wolbachia-positive male and female*. In this case, there is a population of $F(1-\mu)p_t^2$
243 and also a population of $F\mu(1-s_h)p_t^2$ when ova become uninfected due to imperfect
244 maternal transmission, resulting in a population fraction of $F(1-\mu s_h)p_t^2$.

245 2. *Wolbachia-negative male and female*. The population fraction is simply $(1-p_t)^2$.

246 3. *Wolbachia-negative male, Wolbachia-positive female*. Accounting for fecundity in
247 *Wolbachia*-positive females, the population fraction is then $Fp_t(1-p_t)$.

4. *Wolbachia-positive male, Wolbachia-negative female*. The population from generation t is $p_t(1-p_t)$. A fraction $1-s_h$ of this population survives from this incompatible pairing, so the population fraction for generation $t+1$ is $p_t(1-p_t)(1-s_h)$.

Assuming equal infection frequencies in males and females, the adult infection frequency in generation t, denoted p_t, changes between generations as follows:

$$p_{t+1} = \frac{p_t F(1-\mu)}{1 + p_t(F-1-s_h) + p_t^2 s_h(1-\mu F)} \quad [3]$$

(Hoffmann et al. 1990). In the absence of CI ($s_h = 0$), this model becomes

$$p_{t+1} = \frac{p_t F(1-\mu)}{1 + p_t(F-1)}. \quad [4]$$

For a stability analysis of [4], see Appendix 1.

Simulations to approximate temporal Wolbachia dynamics under finite population size

Following Turelli and Barton (2022) and Turelli et al. (2022), we approximated the stochasticity produced by finite population size using a stochastic transition matrix analogous to a haploid Wright-Fisher model of genetic drift, which assumes that generations are discrete and the new generation is a random sample of constant population size drawn from the total number of offspring produced by the previous generation (Crow and Kimura 1970). The model uses an effective population size of N females. The finite-population stochasticity, modeled as binomial sampling, is superimposed on the deterministic equilibria dynamics described by [3]. We explored a range of biologically plausible host population sizes ranging from 10^3 to 10^6 (McKenzie 1980; McInnis et al. 1982; Powell 1997; Gravot et al. 2004; Bergland et al. 2014). Estimates of local population sizes of *Drosophila* made from mark-release-recapture methods report local census sizes on the order of 10^4 to 10^5, with considerable variation among seasons,

268 years, and localities (McKenzie 1980; McInnis et al. 1982; Powell 1997; Gravot et al. 2004;
269 Bergland et al. 2014).

270 We now derive a model for modeling infection frequency p_t of *Wolbachia*-positive hosts
271 which includes randomness effects from a finite female population of size N, $I_t = Np_t$ of which
272 are infected. We assume females produce the same number of eggs with each mating and that N
273 does not change over generations. Starting with the current adult (female) infection frequency p_t,
274 the infection frequency among viable gametes in the next generation is determined by [3]. Then,
275 the infection frequency in the next generation of N adult females is obtained from binomial
276 sampling of this deterministic projection.

277 First, we compute the total number of *Wolbachia*-positive adult offspring in generation
278 $t + 1$ in the absence of CI ($s_h = 0$). For *Wolbachia*-positive females, we note that there are FI_t
279 ova produced. Each ovum has a probability $1 - \mu$ of being infected, so the total number of
280 infected offspring can be represented by a binomial random variable

$$X_t \sim \mathrm{Bin}\big(FI_t, (1-\mu)\big). \qquad [5]$$

281 For the total number of offspring produced, we observe that all *Wolbachia*-negative females
282 produce *Wolbachia*-negative ova. This gives a total of $N - I$ *Wolbachia*-negative offspring for
283 the next generation. For *Wolbachia*-positive females, we noted that FI_t offspring are produced
284 from matings. This gives a total population of $N + (F-1)I_t$ offspring. The proportion of
285 *Wolbachia*-positive adults for generation $t + 1$ is then

$$p_{t+1} = \frac{X_t}{FI_t + N - I_t} = \frac{X_t/N}{p_t(F-1)+1}. \qquad [6]$$

286 From [6], the expected value and variance of p_{t+1}, given knowledge of p_t, are readily computed
287 as

$$\mathbb{E}[p_{t+1}|p_t] = \frac{F(1-\mu)p_t}{p_t(F-1)+1}, \quad \mathrm{Var}(p_{t+1}|p_t) = \frac{F\mu(1-\mu)p_t}{N(p_t(F-1)+1)^2}. \qquad [7]$$

From the law of large numbers, as the population $N \to \infty$, the variance in [7] tends to 0, and the random recursion [6] converges to the deterministic model [4].

Now, allowing for CI ($s_h > 0$), we can derive a random recursion for p_t. For each of the stages of mating, ova production, and the generation of adult offspring, we record total populations in Table S1. The total *Wolbachia*-positive adult offspring resulting from *Wolbachia*-positive male and female matings is given by $X_1 \sim \mathrm{Bin}\big(FpI, (1-\mu)\big)$. For *Wolbachia*-negative males and -positive females, total *Wolbachia*-positive offspring is $X_2 \sim \mathrm{Bin}\big(F(1-p)I, (1-\mu)\big)$. The total number of offspring is found by summing the four terms in the row labeled "adult offspring after CI" in Table S1. Denoting the normalized fractions $\tilde{X}_i = X_i/N$, the fraction of *Wolbachia*-positive offspring over the total population is then

$$p_{t+1} = \frac{\tilde{X}_1+\tilde{X}_2}{s_h(1-F)p_t^2+(F-s_h-1)p_t+s_h\tilde{X}_1+1}. \qquad [8]$$

As $N \to \infty$, from the law of large numbers [8] approaches the deterministic model [3].

Let us also consider the case where a subpopulation of "low transmitter" females with high rates of imperfect maternal transmission are included in the host population. Here, the host population consists of M groups with group fractions $(r_1, \dots, r_M)$. Rather than a single μ value, the ith subpopulation assumes a value μ_i for $i = 1, \dots, M$. To compute *Wolbachia*-positive offspring, we are now summing M separate binomial distributions. However, most computations from above carry over. For each group i, we compute $X_i \sim \mathrm{Bin}(FIr_i, 1-\mu_i)$. The number of *Wolbachia*-positive female eggs then becomes $S^M = \sum_{i=1}^{M} X_i$. For no CI, the total population is still $FI + N - I$, and

$$p_{t+1} = \frac{S_{t+1}^M}{FI_t + N - I_t} = \frac{S_{t+1}^M / N}{p_t(F-1)+1}. \quad [9]$$

When $\mu_i \equiv \mu$ for all $i = 1, \ldots, M$, then $S^M \sim \mathrm{Bin}(1-\mu, FI)$ and we recover [6]. Expected values are also straightforward to compute, with

$$\mathbb{E}[p_{t+1}|p_t] = \frac{F\left(1 - \sum_{i=1}^M \mu_i r_i\right) p_t}{p_t(F-1)+1}. \quad [10]$$

Each of the *Wolbachia*-positive populations X_i for $i \ldots, M$ terms are independent, so by additivity of variance,

$$\mathrm{Var}(p_{t+1}|p_t) = \frac{F\left(\sum_{i=1}^M \mu_i(1-\mu_i) r_i\right) p_t}{N(p_t(F-1)+1)^2}. \quad [11]$$

The stable equilibrium, where $\hat{p} = \mathbb{E}[p_{t+1}|p_t = \hat{p}]$, is very similar to [1]. Accounting for multiple μ_i values, we have

$$\hat{p} = 1 - \frac{F}{F-1} \sum_i \mu_i \, r_i. \quad [12]$$

Finally, to generalize [8], we replace X_1 and X_2 with sums of independent binomials $\{Y_i\}_{1 \le i \le M}$ and $\{Z_i\}_{1 \le i \le M}$, with

$$X_1 = \sum_{i=1}^M Y_i, \qquad Y_i \sim \mathrm{Bin}(Fpr_i I, 1-\mu_i), \quad [13]$$

$$X_2 = \sum_{i=1}^M Z_i, \qquad Z_i \sim \mathrm{Bin}(F(1-p) r_i I, 1-\mu_i). \quad [14]$$

Previous estimates of μ from a large sample of field-collected female *D. santomea* (N = 62) and *D. yakuba* (N = 71) on São Tomé in 2018 suggest the majority of females have perfect or near perfect transmission rates, but a small proportion of low transmitters have high values of μ. For *w*San, the total sample of *Wolbachia*-positive females had a mean value of μ = 0.068 (0.027, 0.154), but 8% of these females had a μ value greater than 0.5 with a mean of μ = 0.728. Similarly, for *w*Yak, the total sample of *Wolbachia*-positive females had a mean value of μ =

321 0.126 (0.062, 0.238), but approximately 11% of the females had a μ value greater than 0.5 with a
322 mean of μ = 0.803 (Hague et al. 2020*a*). Previous work using field-collected females found
323 similar evidence of low transmitters for *w*Mel in *D. melanogaster* (Hoffmann et al. 1998), *w*Suz
324 in *D. suzukii* (Hamm et al. 2014; see Figure 3), *w*Inn in *D. innubila* (Unckless et al. 2009), and
325 *w*Ri in *D. simulans* (Carrington et al. 2011; see Figure 6). Hamm et al. (2014) termed females
326 with high rates of imperfect *w*Suz transmission as "low transmitters" and we follow the same
327 terminology here. Using the 2018 *D. yakuba*-clade *Wolbachia* data as a guide, we explored the
328 effect of treating a 10% subpopulation of *Wolbachia*-positive females as low transmitters with a
329 random binomial μ variable set to μ = 0.8. The rest of the *Wolbachia*-positive females had μ
330 values set as described above ($0.001 \leq \mu \leq 0.5$).
331 While we initial assumed a fixed *F* value, we also considered the case where host fitness
332 effects fluctuate from one host generation to the next as independent, identically distributed log-
333 normal random variables (Turelli et al. 2022). We assume that each generation *F* is chosen
334 independently from a log-normal distribution such that $F = e^X$, where *X* is a normal random
335 variable with mean μ_X and variance σ^2 (Turelli et al. 2022). This implies that *F* has median $m =$
336 e^{μ_x} and a squared coefficient of variation $CV^2 = \mathrm{Var}(F)/[\mathrm{E}(F)^2] = e^{\sigma^2} - 1$. To produce a
337 particular median, *m*, and *CV* for *F*, we set $\mu_x = \ln(m)$ and $\sigma^2 = \ln(CV^2 + 1)$. While it is
338 generally unknown whether host fitness effects fluctuate in natural host populations (Turelli et al.
339 2022), there is evidence that the fitness effects of *w*Mel on *D. melanogaster* fecundity (Kriesner
340 et al. 2016) and virus-blocking (Chrostek et al. 2021) can depend on the environmental context.
341 We explored scenarios with weakly (*CV* = 0.01) and strongly (*CV* = 0.1) fluctuating host fitness
342 effects. To illustrate how these values correspond to fluctuating *F* values in our simulations,

when median(F) = 1.05, a CV = 0.01 value corresponds to 2.5 and 97.5 percentiles of 1.03 and 1.071, respectively, and a CV = 0.1 value corresponds to 0.863 and 1.271, respectively.

We ran a set of 25 simulations for every unique combination of parameters. Each individual simulation began with the arbitrary intermediate *Wolbachia* frequency of $p_0 = 0.4$ and ran for 10,000 host generations (similar p_0 values do not qualitatively alter the results). We removed an initial burn-in of 500 host generations as *Wolbachia* spread from $p_0 = 0.4$ to a stable equilibrium, and then calculated the standard deviation (p_{SD}) and mean ($\bar{p}$) *Wolbachia* frequency from generations 501-10,000 for each simulation. To quantify the influence of the different parameter values on the outcome of simulations, we modeled the p_{SD} and $\bar{p}$ values with linear effects for N, μ, the presence/absence of low transmitters, F, the presence/absence of fluctuating F values (i.e., treating F as fixed or a random variable), and s_h. Since the frequency is always between zero and one, we modeled the distribution of the p_{SD} and $\bar{p}$ values as beta random variables. Models were implemented in R version 4.4.2 using the *mgcv* package version 1.9.1 (Wood 2017). We found that a small handful of simulations had infections that persisted at $p > 0$ for the full 10,000 host generations for combinations of parameter values that do not predict a stable equilibrium of $\hat{p} > 0$ (e.g., $F = 1.05$, $\mu = 0.05$, $s_h = 0$). We removed these simulations from our regression analysis, because they are predicted to be deterministically lost over time and we did not want the p_{SD} and $\bar{p}$ values to bias our analyses of stable equilibria. Finally, we used the "plot_predictions" function from the *marginaleffects* package version 0.25 (Arel-Bundock et al. 2024) to generate model predictions for p_{SD} and $\bar{p}$ as a function of the μ value modulated by the presence/absence of low transmitters, F, and s_h.

366 **RESULTS**

367 We ran 491,400 simulations to examine how different parameter combinations of host
368 population size, imperfect maternal transmission, host fitness effects, and CI contribute to
369 stochastic fluctuations (measured as p_{SD}) and *Wolbachia* equilibria (measured as $\bar{p}$) over time in
370 simulated host populations (Figures S1, S2). Multiple regression was used to summarize how N,
371 μ, F, and s_h impacted p_{SD} (Table 1, Figure 3) and $\bar{p}$ (Table 2, Figure 4) in our simulations. We
372 first explore how different parameters values influence the size of stochastic fluctuations over
373 time (p_{SD}) and then examine how temporal changes to parameter values, particularly the
374 maternal transmission rate, between host generations alter deterministic *Wolbachia* equilibria
375 ($\bar{p}$). For both scenarios, we consider whether the dynamics in our simulations can explain
376 empirical examples of temporally fluctuating *w*Mel-like *Wolbachia* in Australia and São Tomé.

377 All the variables in our regression model had a significant effect on stochastic
378 fluctuations measured as p_{SD}; however, some parameters were more influential than others
379 (Table 1, Figures 3, S1). Notably, host population size had only a small effect ($\beta = -4.14 \times 10^{-7}$, P
380 < 0.001), although p_{SD} generally declined as population size increased and *Wolbachia*
381 frequencies hovered closer to predicted equilibria. Given that host population size had only a
382 minor effect on p_{SD}, we focus here on our results from a single biologically plausible population
383 size of $N = 10^4$ as a simple case to illustrate how other parameters contribute to p_{SD} (Figures 5,
384 S3). Broadly, our results illustrate an intuitive pattern where the parameter values that yield high
385 mean infection frequencies—high rates of maternal transmission, strong fitness benefits, and
386 CI—tend to generate lower p_{SD} values and smaller fluctuations. In contrast, the parameters that
387 yield low infection frequencies ($\bar{p} < 0.2$) typically generate the largest *Wolbachia* fluctuations
388 over time. Within the biologically plausible range of μ, F, and s_h values that we explored, μ had

389 the strongest relative effect on p_{SD} (β = 8.51, P < 0.001), as lower maternal transmission rates
390 (i.e., larger μ values) are associated with lower infection frequencies and larger fluctuations. To a
391 lesser extent, the inclusion of a subpopulation (10%) of low transmitter females (μ = 0.8) also
392 generally increased p_{SD} values (β = 1.12, P < 0.001). Here, we also found an interaction effect
393 between the value of μ and the presence of low transmitters (β = -4.42, P < 0.001), such that the
394 rate of increase in p_{SD} as a function of μ is smaller when low transmitters are present. The value
395 of F had a smaller relative effect on p_{SD} than μ (β = -2.04, P < 0.001), wherein stronger host
396 fitness benefits are associated with higher infection frequencies and smaller fluctuations. If we
397 instead treat F as a log-normal random variable and assume fluctuating host effects, weak
398 fluctuations (CV = 0.01) only had a minor effect on increasing p_{SD} values (β = 0.423, P < 0.001),
399 whereas strong fluctuations predictably had a larger effect (β = 1.78, P < 0.001). Finally, the
400 addition of weak CI at a biologically plausible level for *w*Mel-like *Wolbachia* (s_h = 0.1) had a
401 relatively small effect on p_{SD} values (β = -9.85 x 10^{-2}, P < 0.001). CI generally causes higher
402 infection frequencies and smaller fluctuations. Strong CI characteristic of strains like *w*Ri (s_h =
403 0.45) had a larger effect on p_{SD} (β = -0.783, P < 0.001), as strong CI is associated with high,
404 stable infection frequencies (Figure S3).

405 Can these stochastic dynamics explain empirical observations of temporally fluctuating
406 *w*Mel-like *Wolbachia*? At Gold Coast in Australia, *w*Mel frequencies dropped from p = 0.919
407 (0.787, 0.972) in March 1995 down to p = 0.25 (0.12, 0.449) in April and then back up to p =
408 0.615 (0.355, 0.823) in September, representing a maximum absolute change in frequencies (p_{max}
409 - p_{min}) of 0.669 occurring over just a month-long period (Figure 1). On São Tomé, *w*San
410 frequencies dropped from p = 0.772 (0.648, 0.862) in 2009 to p = 0.368 (0.234, 0.527) in 2015
411 and then back up to p = 0.795 (0.692, 0.87) in 2018, representing a maximum frequency change

412 of 0.427 over the course of a six-year period (Figure 1). Generally, the simulations assuming
413 fixed or weakly fluctuating host effects ($CV = 0.01$) produced small frequency fluctuations that
414 cannot explain *w*Mel or *w*San (Figures 6, S4). Assuming a host population size of $N = 10^4$, we
415 found that the parameter combination of $\mu = 0.1$ (without low transmitters), a fixed value of $F =$
416 1.125, and $s_h = 0.1$ produced the largest frequency fluctuations, with an absolute difference
417 between the maximum and minimum frequency of 0.07 in an individual simulation spanning
418 10,000 host generations. Adding weakly fluctuating host fitness effects ($CV = 0.01$) produced
419 only a slightly larger maximum absolute difference of 0.12 from the parameters $\mu = 0.05$
420 (without low transmitters), $F = 1.05$, and $s_h = 0.1$. Only when we assume strongly fluctuating
421 fitness effects ($CV = 0.1$) do we find large fluctuations that can potentially account for empirical
422 observations of *w*Mel and *w*San. The parameters $\mu = 0.01$ (without low transmitters), $F = 1.025$,
423 and $s_h = 0$ produced the largest absolute frequency difference of 0.855 between $p_{\max}$ and $p_{\min}$
424 over the course of a single simulation (Figure S5).

425 These results highlight a pattern where the specific combination of parameters that
426 generate the largest p_{SD} values does not necessarily align strictly with the general trends outlined
427 above in the regression analysis. In the absence of strong fluctuating host effects, simulations
428 with CI ($s_h = 0.1$) and intermediate values of μ ($0.05 \leq \mu \leq 0.15$) generated the highest p_{SD} values
429 (Figure 5A). With the addition of strong fluctuating host effects, simulations with no CI ($s_h = 0$)
430 and small μ values ($0.005 \leq \mu \leq 0.01$) combined with small F values ($F = 1.025$) generated the
431 highest p_{SD} values (Figure 5B). In this region of parameter space, no CI and the presence of
432 strongly fluctuating F values with a median slightly greater than one cause *Wolbachia* to
433 fluctuate between strongly favored ($F[1 - \mu] > 1$) and disfavored ($F[1 - \mu] < 1$) in the host
434 population (Figure S5). With a median of $F = 1.025$ and $CV = 0.1$, the 2.5 and 97.5 percentiles

435 are 0.843 and 1.251, respectively. Only the simulations with no CI and strong fluctuating host
436 effects ($CV = 0.1$) produced absolute frequency differences ≥ 0.669 in individual simulations that
437 were on the scale of *w*Mel fluctuations observed at Gold Coast. Because the *w*San fluctuations at
438 São Tomé were not quite as large, both the no CI and weak CI simulations with strongly
439 fluctuating host effects produced maximum absolute frequency differences ≥ 0.427 that are
440 comparable to *w*San. Without CI, the presence of a low transmitter subpopulation generally
441 reduced maximum observed frequency differences (Figure 6) and low transmitters cannot be
442 present in order to generate maximum frequency differences ≥ 0.669 comparable to *w*Mel. In
443 fact, the values of $0.005 \leq \mu \leq 0.01$ (without low transmitters), $F = 1.025$ ($CV = 0.1$), and $s_h = 0$
444 were the only combinations of parameters that generated absolute frequency differences ≥ 0.669
445 as observed for *w*Mel at Gold Coast.

446 We also examine how the values of μ, F, and s_h influenced *Wolbachia* equilibria as
447 measured by $\bar{p}$ (Figures 4, S2) to explore the alternative possibility that changes to these
448 parameter values between host generations could generate deterministic increases/decreases in
449 *Wolbachia* frequencies over time that explain *w*Mel-like *Wolbachia* dynamics. Again, we used
450 multiple regression to summarize how different values of N, μ, F, and s_h impacted $\bar{p}$ in our
451 simulations (Table 2). Host population size had a very small relative effect on $\bar{p}$ values ($\beta = -1.58$
452 $\times 10^{-8}$, $P = 0.009$). As expected, our results otherwise align tightly with equilibria predictions
453 from the strictly deterministic model (Figure 2), which shows that high rates of transmission
454 (smaller μ values), strong beneficial host effects (larger F values), and strong CI (larger s_h
455 values) yield high equilibrium frequencies. Within the biologically plausible range of parameters
456 we explored, the value of μ had the strongest relative effect on $\bar{p}$ ($\beta = -22.4$, $P < 0.001$). To a
457 lesser extent, the inclusion of a subpopulation of low transmitter females was also associated

with lower $\bar{p}$ values (β = -2.43, $P < 0.001$). We also found an interaction effect between the μ value and the presence of low transmitters (β = 8.26, $P < 0.001$), such that the rate of decrease in $\bar{p}$ as a function of μ is slightly less when low transmitters are present. The value of F had a smaller relative effect on $\bar{p}$ compared to μ (β = 3.77, $P < 0.001$) and the addition of fluctuating host fitness effects had only a minor effect on $\bar{p}$ (CV = 0.01: $\beta = 1.30 \times 10^{-4}$, P = 0.961; CV = 0.1: $\beta = 9.68 \times 10^{-3}$, $P < 0.001$). Finally, the addition of weak CI had a small effect on $\bar{p}$ (β = 0.427, $P < 0.001$), whereas strong CI had a much stronger effect (β = 1.92, $P < 0.001$), as the frequency dependent benefit of CI drives *Wolbachia* to high equilibrium frequencies.

While including a subpopulation of low transmitters (μ = 0.8) generally reduced $\bar{p}$ values, we note that this effect was strongest for *Wolbachia* strains that do not cause CI (Figures 4, S2). Again, we focus on the simple case of $N = 10^4$ to illustrate how different parameter values contribute to $\bar{p}$ (Figures 5, S3). Here, with no CI (s_h = 0), the median $\bar{p}$ value dropped from 0.807 for all our simulations with a strictly binomial μ value to 0.472 for the simulations that included a low transmitter subpopulation. In contrast, the median $\bar{p}$ value dropped from 0.875 to 0.591 with low transmitters for weak CI (s_h = 0.1) and from 0.945 to 0.858 for strong CI (s_h = 0.45). The impact of low transmitters on $\bar{p}$ is especially strong for relatively small values of μ ($\leq$ 0.01) and F ($\leq$ 1.15), which are otherwise predicted to generate high equilibrium frequencies (Figure 2). For instance, the values of μ = 0.001, F = 1.1, and s_h = 0 generated a pooled mean of $\bar{\bar{p}}$ = 0.989 across the set of 25 simulations, but the addition of low transmitters dropped the mean down to $\bar{\bar{p}}$ = 0.11.

Can changes to the maternal transmission rate or the presence of low transmitters between host generations generate large deterministic drops in *Wolbachia* frequencies over time on the scale observed for *w*Mel-like *Wolbachia*? We further examined the $\bar{\bar{p}}$ values from our

simulations (Figure 5C) to infer how changes to μ, F, or s_h between host generation could alter equilibrium frequencies over time. We found that a range of parameter values could plausibly explain the drop in *w*Mel frequencies from $p = 0.919$ in March down to $p = 0.25$ in April of 1995 at Gold Coast if we assume that changes to μ values or the presence of low transmitters occur between host generations (Figures S6). For instance, the values of $\mu = 0.005$, $F = 1.075$, and $s_h = 0$ produced a value of $\bar{\bar{p}} = 0.928$, which falls within the confidence interval of p for *w*Mel in March. Then, assuming a drop in the transmission rate to $\mu = 0.05$ in subsequent generations (while all else remains equal), *Wolbachia* frequencies drop to $\bar{\bar{p}} = 0.283$, which falls within the confidence interval of p in April (Figure S7). Or, assuming the values of $\mu = 0.005$, $F = 1.125$, and $s_h = 0$ in March ($\bar{\bar{p}} = 0.955$), and then adding a subpopulation of low transmitters in April ($\bar{\bar{p}} = 0.239$) could also explain the drop. Of course, subtle changes in multiple parameters, including F and s_h, could also explain the temporal drop in frequencies. For example, the values of $\mu = 0.01$, $F = 1.025$, and $s_h = 0.1$ could explain March ($\bar{\bar{p}} = 0.920$) and then a slight decrease in the maternal transmission rate, increase in host fitness effects, and the loss of CI ($\mu = 0.05$, $F = 1.075$, and $s_h = 0$) could explain April ($\bar{\bar{p}} = 0.283$).

We found that a similar range of parameter values could plausibly explain the drop in *w*San from $p = 0.772$ in 2009 to $p = 0.368$ in 2015 on São Tomé (Figure S8). For instance, the values of $\mu = 0.01$, $F = 1.075$, and $s_h = 0$ produced a value of $\bar{\bar{p}} = 0.857$, which falls within the confidence interval of p for *w*San in 2009. Then, assuming a drop in the transmission rate to $\mu = 0.05$ (while all else remains equal), *Wolbachia* frequencies drop to $\bar{\bar{p}} = 0.283$, falling within the 2015 p estimate (Figure S9). Assuming the addition of low transmitters in 2015 could also plausibly explain the drop in *Wolbachia* frequencies. For example, the values of $\mu = 0.05$, $F = 1.175$, and $s_h = 0.1$ produced $\bar{\bar{p}} = 0.782$, and could explain 2009, and then adding a subpopulation

504 of low transmitters drops *Wolbachia* frequencies to $\bar{\bar{p}} = 0.284$, falling within the 2015 p estimate.
505 Subtle changes in multiple parameters could also plausibly explain the drop in frequencies. For
506 instance, the values of $\mu = 0.005$, $F = 1.025$, and $s_h = 0$ produced $\bar{\bar{p}} = 0.795$ and could explain
507 2009, whereas a slight drop in the maternal transmission rate and increase in host fitness effects
508 ($\mu = 0.05$, $F = 1.075$, and $s_h = 0$) produced $\bar{\bar{p}} = 0.283$ and could explain 2015.
509

510 **DISCUSSION**

511 We explored how finite host population size in conjunction with maternal transmission
512 rates, host fitness effects, and CI contribute to the temporal dynamics of *w*Mel-like *Wolbachia*.
513 Broadly, we find that strains like *w*Mel and *w*San that cause no or weak CI are more likely to
514 generate large stochastic fluctuations over time than strains like *w*Ri that cause strong CI. The
515 combination of no CI, host effects that fluctuate between mutualistic and deleterious, and a
516 modest maternal transmission rate generated the absolute largest stochastic fluctuations over
517 time in our model, regardless of population size. Changes between host generations to the
518 maternal transmission rate or the presence/absence of low transmitters can also generate large
519 deterministic changes to *Wolbachia* frequencies, as can between-generation changes to host
520 fitness effects and CI. The results suggest that stochastic dynamics and/or between-generation
521 changes to parameter values can provide plausible explanations for the temporal fluctuations of
522 *w*San on São Tomé over years-long periods, but the fluctuations of *w*Mel at Gold Coast are more
523 difficult to explain in the context of our model.

524 We first evaluated whether finite-population stochasticity alone can explain the temporal
525 dynamics of *w*Mel-like *Wolbachia*. Assuming the values of μ, F, and s_h remain fixed over time,
526 we found that stochasticity in our model generates only minor fluctuations over time, regardless

527 of host population size. Even small host population sizes (10^3) were generally outweighed by
528 deterministic dynamics, as *Wolbachia* frequencies tend to fluctuate closely around predicted
529 equilibria. Notably, across all the biologically plausible parameter values that we explored, poor
530 rates of maternal transmission (i.e., increasing values of μ) had the strongest relative effect on
531 increasing *Wolbachia* fluctuations in our simulations (Table 1). However, very specific
532 conditions were required to generate the absolute largest frequency fluctuations. Assuming fixed
533 host fitness effects, weak-CI causing *Wolbachia* ($s_h = 0.1$) with moderate fitness benefits (1.125
534 $\leq F \leq 1.2$) and relatively poor rates of maternal transmission ($0.1 \leq \mu \leq 0.2$) generated that
535 largest p_{SD} values (Figure 5A). Adding a subpopulation of low transmitters generally increased
536 the size of fluctuations; however, low transmitters were not present in the simulations that
537 produced the largest p_{SD} values. Only the addition of strongly fluctuating host fitness effects (CV
538 $= 0.1$) under a limited set of conditions can replicate fluctuations on the scale of *w*Mel-like
539 *Wolbachia*, particularly for *w*Mel at Gold Coast in Australia. Here, non-CI causing *Wolbachia*
540 with median F values close to one ($1.025 \leq F \leq 1.075$) combined with a high fidelity of
541 transmission ($0.005 \leq \mu \leq 0.05$) generated the largest p_{SD} values (Figure 5B), as *Wolbachia*
542 fluctuate between mutualistic ($F[1 - \mu] > 1$) and deleterious ($F[1 - \mu] < 1$) (Figure S5). In
543 contrast, conditions that yield equilibrium frequencies near one—strong CI, near perfect
544 maternal transmission, and large host fitness benefits—generate smaller stochastic fluctuations
545 over time.

546 These results are generally consistent with empirical observations of *Wolbachia*
547 frequency fluctuations in natural populations. *w*Mel-like *Wolbachia* that cause no or weak CI and
548 are imperfectly transmitted in nature tend to show evidence of temporally and/or spatially
549 fluctuating *Wolbachia* frequencies (Hoffmann et al. 1994; Kriesner et al. 2016; Cooper et al.

550 2017). Estimates of CI for *w*Mel using crosses between field-collected male *D. melanogaster*
551 from Australia and *Wolbachia*-negative laboratory females are consistent with $s_h \approx 0$ (unless
552 males are very young) (Hoffmann et al. 1998; Reynolds and Hoffmann 2002; Kriesner et al.
553 2016; Shropshire et al. 2021). Estimates of *w*Mel maternal transmission rates from field-
554 collected females have been recorded as high $\mu = 0.11$ (0.07, 0.17) (Olsen et al. 2001). Similar
555 levels of imperfect maternal transmission have also been recorded for *w*San from field-collected
556 *D. santomea* ($\mu = 0.120$, [0.032, 0.346]) and for *w*Yak from *D. yakuba* ($\mu = 0.20$ [0.087, 0.364])
557 on São Tomé (Hague et al. 2020*b*). Importantly, these patterns are not strictly characteristic of all
558 "*w*Mel-like" *Wolbachia*, as some *w*Mel-like strains cause strong CI in their native hosts (e.g.,
559 *w*Seg in *D. seguyi*; Shropshire et al. 2024) and other *Wolbachia* such as the *w*Ri-like strain *w*Suz
560 in *D. suzukii* do not cause CI, show imperfect transmission in the field ($\mu = 0.14$ [0.04, 0.27]),
561 and fluctuate across geographic space (Hamm et al. 2014; Turelli et al. 2018). The patterns for
562 non-CI causing *Wolbachia* contrast empirical observations of the *w*Ri strain in *D. simulans*,
563 which causes strong CI ($s_h \approx 0.45$) and tends to persist at high, stable infection frequencies. *w*Ri
564 also seems to have relatively high rates of maternal transmission in the field (e.g., $\mu = 0.026$
565 [0.004, 0.057]) and in the lab at different temperatures (Hoffmann et al. 1990; Turelli and
566 Hoffmann 1995; Carrington et al. 2011; Kriesner et al. 2013; Hague et al. 2024). Similarly, the
567 CI-causing strains *w*Ha (in *D. simulans*) and *w*Ana (in *D. ananassae*) persist at high, stable
568 infection frequencies (Rousset and Solignac 1995; Bourtzis et al. 1996; James and Ballard 2000;
569 Ballard 2004; Choi et al. 2015) and have thermally stable maternal transmission rates in the lab
570 (Hague et al. 2024).

571 It is important to note that strongly fluctuating host fitness effects are required as a
572 condition to generate stochastic fluctuations on the scale of *w*Mel at Gold Coast or *w*San at São

573 Tomé (Figure 6). Unfortunately, we have a poor understanding of *Wolbachia* effects on host
574 fitness in nature, although the endosymbionts are generally considered to be beneficial based on
575 the spread and persistence of *Wolbachia* in nature (Weeks et al. 2007; Hamm et al. 2014; Cooper
576 et al. 2017; Meany et al. 2019; Ross et al. 2019*b*; Hague et al. 2020*b*, 2022; Hoffmann and
577 Cooper 2024). We do not know if host fitness effects fluctuate in nature (Turelli et al. 2022), but
578 there is evidence that the effects of *w*Mel on *D. melanogaster* fecundity (Kriesner et al. 2016)
579 and virus-blocking (Chrostek et al. 2021) can depend on the environmental context. The non-CI
580 causing strain *w*Au in *D. simulans* has also been shown to have context-dependent host effects
581 depending on where host breeding occurs (Cao et al. 2019). Given that temperature has pervasive
582 effects on *Wolbachia* densities in host tissues (Hague et al. 2020*a*, 2024), temperature-induced
583 changes to *Wolbachia* densities could in turn alter *Wolbachia* effects on various host fitness
584 components. The strongly fluctuating host effects we modeled here may also help explain
585 altitudinal variation in *w*Yak frequencies in *D. yakuba* observed on São Tomé in 2018, which
586 otherwise requires invoking unrealistic values of F and s_h (Figure S10; see Hague et al. 2020 for
587 further discussion).

588 Our simulations build on previous work focused on the role of finite-population
589 stochasticity in the initial establishment of *Wolbachia* from low frequencies in host populations
590 (Jansen et al. 2008). At low initial frequencies, *Wolbachia* that generate $F(1 - \mu) > 1$ may be
591 stochastically lost and, conversely, CI-causing strains that generate $F(1 - \mu) < 1$ may become
592 established; however, these probabilities decreases as host population size increases (Rigaud and
593 Rousset 1996; Egas et al. 2002; Jansen et al. 2008). *Wolbachia* that generate $F(1 - \mu) < 1$ are
594 disfavored by selection; however, strong-CI causing *Wolbachia* may still become established if
595 stochastic fluctuations carry *Wolbachia* above the critical threshold frequency at which CI favors

596 infection spread. This is especially relevant for biocontrol programs using transinfected *Aedes*
597 *aegypti* mosquitoes, because *w*Mel is deleterious but also generates strong CI in the mosquito
598 background (Ross et al. 2019*b*). Stochastic dynamics can also cause deleterious infections to be
599 lost if *Wolbachia* fluctuate back below the threshold frequency and they are no longer favored by
600 CI (Jansen et al. 2008). Our simulations here reflect the fact that *Wolbachia* infections in natural
601 hosts are now generally thought to generate $F(1 - \mu) > 1$ (Hoffmann and Turelli 1997; Kriesner
602 et al. 2013, 2016; Hamm et al. 2014; Kriesner and Hoffmann 2018; Meany et al. 2019).
603 We also considered the hypothesis that changes to maternal transmission rates, host
604 fitness effects, and/or CI between host generations could cause deterministic changes to
605 *Wolbachia* frequencies over time that resemble *w*Mel-like *Wolbachia* in nature. Predictably, the
606 $\bar{p}$ values from our simulations (Figures 5C) closely align with equilibria from the deterministic
607 model (Figure 2) (Hoffmann et al. 1990); although, we also considered the addition of low
608 transmitters to the population. Generally, moderate changes to maternal transmission rates (e.g.,
609 $\mu = 0.005$ to 0.05) and/or the addition of low transmitters between host generations can plausibly
610 explain drops in the frequencies of *w*Mel-like *Wolbachia*. Moderate changes to host fitness
611 effects (e.g., $F = 1.025$ to 1.075) and CI strength (e.g., $s_h = 0.1$ to 0) can also cause similar
612 changes to infection frequencies over time. These parameter values generally fall within a
613 biologically plausible range based on aforementioned estimates from field-collected *Drosophila*
614 hosts (Hoffmann et al. 1998, 1998; Olsen et al. 2001; Reynolds and Hoffmann 2002; Kriesner et
615 al. 2016; Shropshire et al. 2021), especially considering that maternal transmission rates of *w*Mel
616 and *D. yakuba*-clade *Wolbachia* can change depending on thermal conditions (Hague et al.
617 2020*b*, 2022, 2024). Of course, it is important to note that our simplified model treats μ, F, and s_h
618 as discrete values from one host generation to the next, whereas these parameters are much more

619 likely to exhibit quantitative variation on a continuous scale in natural populations with
620 overlapping host generations.

621 By incorporating a subpopulation of low transmitters into our simulations, we considered
622 the possibility that maternal transmission rates vary among hosts individuals within a given host
623 generation. This phenomenon has been observed for a number of *Wolbachia* strains in natural
624 host populations, including *w*Mel, *w*San, and *w*Yak (Hoffmann et al. 1998; Carrington et al.
625 2011; Hamm et al. 2014; Hague et al. 2020*b*). The presence of low transmitters caused the
626 largest drops in *Wolbachia* frequencies for strains that do not cause CI (Figure 4). These results
627 imply that heterogeneity of transmission rates among females and changes to the
628 presence/absence of low transmitters between host generations may provide another plausible
629 explanation for *w*Mel-like *Wolbachia* fluctuations over time.

630 Why might some hosts be low transmitters? Heterogeneity in transmission rates could
631 arise within a generation if host individuals experience different thermal conditions that impact
632 maternal transmission rates and *Wolbachia* densities (Ulrich et al. 2016; Ross et al. 2017, 2019*a*;
633 Foo et al. 2019; Hague et al. 2020*b*, 2020*a*, 2022, 2024; Chrostek et al. 2021). Insects are
634 ectotherms that inhabit complex, heterogeneous environments where thermal conditions can vary
635 on the scale of individual fruits or leaves (Roberts and Feder 2000; Potter et al. 2009; Saudreau
636 et al. 2009; Pincebourde and Woods 2012; Woods et al. 2015). Insects thermoregulate
637 behaviorally, but the immobile egg and pupal stages of development leave hosts more
638 susceptible to local microclimatic conditions that could influence maternal transmission or
639 *Wolbachia* densities (May 1979; Heinrich 1993; Dillon et al. 2009; Rajpurohit and Schmidt
640 2016). Heterogeneity of *Wolbachia* densities in hosts could also arise for other reasons, for
641 example, due to individual variation in diet (Serbus et al. 2015; Christensen et al. 2019), age

642 (Reynolds and Hoffmann 2002; Shropshire et al. 2021), and the host and *Wolbachia* genomes
643 (Gu et al. 2022; Hague et al. 2022). For instance, the density of *w*Inn, a strain related to *w*Mel
644 and *w*San, varied by 20,000 fold among host individuals in natural populations of *D. innubila* in
645 Arizona (Dyer and Jaenike 2004; Unckless et al. 2009; Hill et al. 2019).

646 We must point out that our discrete generation model generally requires a number of host
647 generations to achieve stochastic or deterministic changes to *Wolbachia* frequencies over time on
648 the order ≥ 0.669 for *w*Mel and ≥ 0.427 for *w*San (Figures S5, S7, S9). These timescales may be
649 plausible for *w*San on São Tomé, where frequencies fluctuated on the scale of years; however, it
650 is implausible for *w*Mel at Gold Coast, where frequencies fluctuated over just a month-long
651 period. This period from March to April corresponds to roughly a single host generation in the
652 field (Turelli and Hoffmann 1995; Hoffmann et al. 1998). Conservatively, the maximum
653 stochastic change in *Wolbachia* frequences (p_{max} - p_{min}) we observed over five consecutive host
654 generations in our simulations was 0.209 using the parameters that generated the largest p_{SD}
655 values (μ = 0.01, F = 1.025, CV = 0.1, s_h = 0) (see Appendix 2 for a detailed analysis of
656 stochasticity over many host generations). Even if we assume an implausibly small host
657 population of N = 100, the maximum absolute change in *Wolbachia* frequencies that we observe
658 over five consecutive generations is 0.224 in a set of 25 simulations using the aforementioned
659 parameters. If we instead assume that μ, F, and/or s_h values change between host generations, it
660 takes roughly 50 host generations for deterministic changes in equilibria to occur (Figures S7,
661 S9). These results suggest that between-generation changes to maternal transmission, host fitness
662 effects, or CI cannot yield large deterministic changes to *Wolbachia* frequencies over a single
663 host generation according to the assumptions of our model.

664 What else could potentially explain large temporal fluctuations in *Wolbachia* frequencies
665 over just one or two host generations? Importantly, our model assumes that hosts have discrete
666 generations and a fixed population size. Accounting for aspects of insect population dynamics
667 and ecology, such as overlapping generations, density-dependent population regulation, or
668 seasonal variation in population size could also contribute to fluctuating *Wolbachia* frequencies
669 over time (Rasgon and Scott 2004; Farkas and Hinow 2010; Turelli 2010; Hancock et al. 2011;
670 Turelli and Barton 2022). Host migration among structured populations with different *Wolbachia*
671 frequencies could also plausibly alter frequencies within a given focal population (Hoffmann et
672 al. 1998; Flor et al. 2007; Jansen et al. 2008; Engelstädter and Telschow 2009; Haygood and
673 Turelli 2009; Hancock et al. 2011). *Wolbachia* frequencies could potentially vary on small
674 geographic scales due to the effects of microclimatic variation on μ, F, and s_h. At Gold Coast, *D.*
675 *melanogaster* hosts were sampled from 20-25 banana mash buckets along transects of at least 3
676 km. Perhaps microclimatic differences along the transect generated complex variation in
677 *Wolbachia* frequencies (Roberts and Feder 2000; Potter et al. 2009; Saudreau et al. 2009;
678 Pincebourde and Woods 2012; Woods et al. 2015). It is also conceivable that environmental
679 conditions could cause *Wolbachia* frequencies to change within a single host generation if there
680 are extreme effects on *Wolbachia* densities (e.g., a heat wave) that effectively clear *Wolbachia*
681 from some hosts (Ross et al. 2019*a*, 2020).
682 In summary, we find that stochasticity or between-generation changes to the maternal
683 transmission rate (as well as host effects and CI) can provide plausible explanations for the
684 temporal fluctuations of *w*Mel-like *Wolbachia* over years-long periods, but not shorter month-
685 long timescales. Our results highlight the need for future work to explore the scale of temporal
686 and geographic variation of *w*Mel-like *Wolbachia* frequencies in nature, in conjunction with

insect population dynamics (e.g., census population size, migration). It is unclear, for example, whether *Wolbachia* frequencies vary temporally on a scale of less than a month or geographically on the scale of kilometers. Interestingly, the temporal dynamics of *w*Mel at Gold Coast seem to be quite variable, but on a broader geographic scale, *w*Mel frequencies have persisted as a stable latitudinal cline for decades along the coast of eastern Australia (Hoffmann et al. 1994, 1998; Kriesner et al. 2016). In the future, field estimates of maternal transmission rates, fecundity, and CI using wild-caught flies sampled at different temporal and geographic scales can be used to model *Wolbachia* dynamics using the publicly available R package *wlbcmodeler*. Uncovering sources of temporal and geographic variation in *Wolbachia* prevalence is ultimately critical for the understanding the long-term evolutionary dynamics of these host-endosymbiont relationships.

DATA ACCESSIBILITY STATEMENT

The *wlbcmodeler* R package and scripts to recreate figures will be made publicly available upon publication.

COMPETING INTERESTS STATEMENT

The authors declare no competing interests.

AUTHOR CONTRIBUTIONS

JMG: funding acquisition (equal), methodology (equal), formal analysis (lead), software (lead), visualization (lead), writing – original draft (supporting), writing – review and editing (supporting). JK: methodology (equal), formal analysis (supporting), writing – original draft

(supporting), writing – review and editing (supporting). MTJH: funding acquisition (equal), conceptualization (lead), supervision (lead), writing – original draft (lead), writing – review and editing (lead).

ACKNOWLEDGEMENTS

This work was supported by the University of Scranton through a Faculty Internal Research Award to JMG and MTJH and a startup package awarded to MTJH from the College of Arts and Sciences Dean's Office.

LITERATURE CITED

Arel-Bundock, V., N. Greifer, and A. Heiss. 2024. How to Interpret Statistical Models Using marginaleffects for R and Python. Journal of Statistical Software 111:1–32.

Bakovic, V., M. Schebeck, A. Telschow, C. Stauffer, and H. Schuler. 2018. Spatial spread of *Wolbachia* in *Rhagoletis cerasi* populations. Biology Letters 14:20180161.

Ballard, J. W. O. 2004. Sequential evolution of a symbiont inferred from the host: *Wolbachia* and *Drosophila simulans*. Molecular Biology and Evolution 21:428–442.

Bennett, G. M., Y. Kwak, and R. Maynard. 2024. Endosymbioses have shaped the evolution of biological diversity and complexity time and time again. Genome Biology and Evolution evae112.

Bergland, A. O., E. L. Behrman, K. R. O'Brien, P. S. Schmidt, and D. A. Petrov. 2014. Genomic evidence of rapid and stable adaptive oscillations over seasonal time scales in *Drosophila*. PLoS Genetics 10:e1004775.

Bordenstein, S. R., and S. R. Bordenstein. 2011. Temperature affects the tripartite interactions between bacteriophage WO, *Wolbachia*, and cytoplasmic incompatibility. PLoS One 6.

Bourtzis, K., A. Nirgianaki, G. Markakis, and C. Savakis. 1996. *Wolbachia* infection and cytoplasmic incompatibility in *Drosophila* species. Genetics 144:1063–1073.

Brownlie, J. C., B. N. Cass, M. Riegler, J. J. Witsenburg, I. Iturbe-Ormaetxe, E. A. McGraw, and S. L. O'Neill. 2009. Evidence for metabolic provisioning by a common invertebrate endosymbiont, *Wolbachia pipientis*, during periods of nutritional stress. PLoS Pathogens 5:e1000368.

Bruner-Montero, G., and F. M. Jiggins. 2023. *Wolbachia* protects *Drosophila melanogaster* against two naturally occurring and virulent viral pathogens. Scientific Reports 13:8518.

Cao, L.-J., W. Jiang, and A. A. Hoffmann. 2019. Life history effects linked to an advantage for *w*Au *Wolbachia* in *Drosophila*. Insects 10:126.

Carrington, L. B., J. R. Lipkowitz, A. A. Hoffmann, and M. Turelli. 2011. A re-examination of *Wolbachia*-induced cytoplasmic incompatibility in California *Drosophila simulans*. PLoS One 6:e22565.

Caspari, E., and G. Watson. 1959. On the evolutionary importance of cytoplasmic sterility in mosquitoes. Evolution 13:568–570.

Choi, J. Y., J. E. Bubnell, and C. F. Aquadro. 2015. Population genomics of infectious and integrated *Wolbachia pipientis* genomes in *Drosophila ananassae*. Genome biology and evolution 7:2362–2382.

Christensen, S., M. Camacho, Z. Sharmin, A. Z. Momtaz, L. Perez, G. Navarro, J. Triana, et al. 2019. Quantitative methods for assessing local and bodywide contributions to *Wolbachia* titer in maternal germline cells of *Drosophila*. BMC Microbiology 19:1–17.

Chrostek, E., N. Martins, M. S. Marialva, L. Teixeira, N. A. Moran, and N. Dubilier. 2021. *Wolbachia*-Conferred Antiviral Protection Is Determined by Developmental Temperature. mBio 12:e02923-20.

Clancy, D. J., and A. A. Hoffmann. 1998. Environmental effects on cytoplasmic incompatibility and bacterial load in *Wolbachia*-infected *Drosophila simulans*. Entomologia Experimentalis et Applicata 86:13–24.

Cogni, R., S. D. Ding, A. C. Pimentel, J. P. Day, and F. M. Jiggins. 2021. *Wolbachia* reduces virus infection in a natural population of *Drosophila*. Communications Biology 4:1–7.

Conner, W. R., M. L. Blaxter, G. Anfora, L. Ometto, O. Rota-Stabelli, and M. Turelli. 2017. Genome comparisons indicate recent transfer of *w*Ri-like *Wolbachia* between sister species *Drosophila suzukii* and *D. subpulchrella*. Ecology and Evolution 7:9391–9404.

Cooper, B. S., P. S. Ginsberg, M. Turelli, and D. R. Matute. 2017. *Wolbachia* in the *Drosophila yakuba* complex: Pervasive frequency variation and weak cytoplasmic incompatibility, but no apparent effect on reproductive isolation. Genetics 205:333–351.

Cooper, B. S., D. Vanderpool, W. R. Conner, D. R. Matute, and M. Turelli. 2019. *Wolbachia* acquisition by *Drosophila yakuba*-clade hosts and transfer of incompatibility loci between distantly related *Wolbachia*. Genetics 212:1399–1419.

Corbin, C., E. R. Heyworth, J. Ferrari, and G. D. Hurst. 2017. Heritable symbionts in a world of varying temperature. Heredity 118:10–20.

Crow, J. F., and M. Kimura. 1970. An Introduction to Population Genetics Theory. Harper & Row, New York.

Dillon, M. E., G. Wang, P. A. Garrity, and R. B. Huey. 2009. Thermal preference in *Drosophila*. Journal of Thermal Biology 34:109–119.

Dyer, K. A., and J. Jaenike. 2004. Evolutionarily stable infection by a male-killing endosymbiont in Drosophila innubila: molecular evidence from the host and parasite genomes. Genetics 168:1443–1455.

Egas, M., F. Vala, and J. Breeuwer. 2002. On the evolution of cytoplasmic incompatibility in haplodiploid species. Evolution 56:1101–1109.

Engelstädter, J., and A. Telschow. 2009. Cytoplasmic incompatibility and host population structure. Heredity 103:196–207.

Farkas, J. Z., and P. Hinow. 2010. Structured and unstructured continuous models for *Wolbachia* infections. Bulletin of mathematical biology 72:2067–2088.

Ferri, E., O. Bain, M. Barbuto, C. Martin, N. Lo, S. Uni, F. Landmann, et al. 2011. New insights into the evolution of *Wolbachia* infections in filarial nematodes inferred from a large range of screened species. PLoS One 6:e20843.

Fisher, R. M., L. M. Henry, C. K. Cornwallis, E. T. Kiers, and S. A. West. 2017. The evolution of host-symbiont dependence. Nature Communications 8:1–8.

Flor, M., P. Hammerstein, and A. Telschow. 2007. *Wolbachia*-induced unidirectional cytoplasmic incompatibility and the stability of infection polymorphism in parapatric host populations. Journal of Evolutionary Biology 20:696–706.

Foo, I. J.-H., A. A. Hoffmann, and P. A. Ross. 2019. Cross-generational effects of heat stress on fitness and *Wolbachia* density in *Aedes aegypti* mosquitoes. Tropical Medicine and Infectious Disease 4:13.

Fry, A., M. Palmer, and D. Rand. 2004. Variable fitness effects of *Wolbachia* infection in *Drosophila melanogaster*. Heredity 93:379.

Gerth, M., and C. Bleidorn. 2017. Comparative genomics provides a timeframe for *Wolbachia* evolution and exposes a recent biotin synthesis operon transfer. Nature Microbiology 2:16241.

Gravot, E., M. Huet, and M. Veuille. 2004. Effect of breeding structure on population genetic parameters in *Drosophila*. Genetics 166:779–788.

Gu, X., P. A. Ross, J. Rodriguez-Andres, K. L. Robinson, Q. Yang, M.-J. Lau, and A. A. Hoffmann. 2022. A *w*Mel *Wolbachia* variant in *Aedes aegypti* from field-collected *Drosophila melanogaster* with increased phenotypic stability under heat stress. Environmental Microbiology 24:2119–2135.

Hague, M. T., C. N. Caldwell, and B. S. Cooper. 2020*a*. Pervasive effects of *Wolbachia* on host temperature preference. mBio 11:e01768-20.

Hague, M. T. J., J. D. Shropshire, C. N. Caldwell, J. P. Statz, K. A. Stanek, W. R. Conner, and B. S. Cooper. 2022. Temperature effects on cellular host-microbe interactions explain continent-wide endosymbiont prevalence. Current Biology 32:878-888.e8.

Hague, M. T. J., H. A. Woods, and B. S. Cooper. 2021. Pervasive effects of *Wolbachia* on host activity. Biology Letters 17:20210052.

Hague, M. T., H. Mavengere, D. R. Matute, and B. S. Cooper. 2020*b*. Environmental and genetic contributions to imperfect *w*Mel-like *Wolbachia* transmission and frequency variation. Genetics 215:1117–1132.

Hague, M. T., T. B. Wheeler, and B. S. Cooper. 2024. Comparative analysis of *Wolbachia* maternal transmission and localization in host ovaries. Communications Biology 7:727.

Hamm, C. A., D. J. Begun, A. Vo, C. C. Smith, P. Saelao, A. O. Shaver, J. Jaenike, et al. 2014. *Wolbachia* do not live by reproductive manipulation alone: Infection polymorphism in *Drosophila suzukii* and *D. subpulchrella*. Molecular Ecology 23:4871–4885.

Hancock, P. A., S. P. Sinkins, and H. C. J. Godfray. 2011. Population dynamic models of the spread of *Wolbachia*. The American Naturalist 177:323–333.

Haygood, R., and M. Turelli. 2009. Evolution of incompatibility-inducing microbes in subdivided host populations. Evolution 63:432–447.

Hedges, L. M., J. C. Brownlie, S. L. O'Neill, and K. N. Johnson. 2008. *Wolbachia* and virus protection in insects. Science 322:702–702.

Heinrich, B. 1993. The hot-blooded insects: strategies and mechanisms of thermoregulation. Harvard University Press.

Hill, T., B. S. Koseva, and R. L. Unckless. 2019. The genome of *Drosophila innubila* reveals lineage-specific patterns of selection in immune genes. Molecular Biology and Evolution 36:1405–1417.

Hoffmann, A. A., D. J. Clancy, and E. Merton. 1994. Cytoplasmic incompatibility in Australian populations of *Drosophila melanogaster*. Genetics 136:993–999.

Hoffmann, A. A., and B. S. Cooper. 2024. Describing endosymbiont–host interactions within the parasitism–mutualism continuum. Ecology and Evolution 14:e11705.

838 Hoffmann, A. A., M. Hercus, and H. Dagher. 1998. Population dynamics of the *Wolbachia*
839 infection causing cytoplasmic incompatibility in *Drosophila melanogaster*. Genetics 148:221–
840 231.

841 Hoffmann, A. A., and M. Turelli. 1997. Cytoplasmic incompatibility in insects. Pages 42–80 *in*
842 S. L. O'Neill, A. A. Hoffmann, and J. H. Werren, eds. Influential passengers: inherited
843 microorganisms and arthropod reproduction. Oxford University Press.

844 Hoffmann, A. A., M. Turelli, and L. G. Harshman. 1990. Factors affecting the distribution of
845 cytoplasmic incompatibility in *Drosophila simulans*. Genetics 126:933–948.

846 Hoffmann, A., and M. Turelli. 1988. Unidirectional incompatibility in *Drosophila simulans*:
847 inheritance, geographic variation and fitness effects. Genetics 119:435–444.

848 James, A. C., and J. W. O. Ballard. 2000. Expression of cytoplasmic incompatibility in
849 *Drosophila simulans* and its impact on infection frequencies and distribution of *Wolbachia*
850 *pipientis*. Evolution 54:1661–1672.

851 Jansen, V. A. A., M. Turelli, and H. C. J. Godfray. 2008. Stochastic spread of *Wolbachia*.
852 Proceedings of the Royal Society of London B: Biological Sciences 275:2769–2776.

853 Kriesner, P., W. R. Conner, A. R. Weeks, M. Turelli, and A. A. Hoffmann. 2016. Persistence of
854 a *Wolbachia* infection frequency cline in *Drosophila melanogaster* and the possible role of
855 reproductive dormancy. Evolution 70:979–997.

856 Kriesner, P., and A. A. Hoffmann. 2018. Rapid spread of a *Wolbachia* infection that does not
857 affect host reproduction in *Drosophila simulans* cage populations. Evolution 72:1475–1487.

858 Kriesner, P., A. A. Hoffmann, S. F. Lee, M. Turelli, and A. R. Weeks. 2013. Rapid sequential
859 spread of two *Wolbachia* variants in *Drosophila simulans*. PLoS Pathogens 9:e1003607.

860 Martinez, J., B. Longdon, S. Bauer, Y.-S. Chan, W. J. Miller, K. Bourtzis, L. Teixeira, et al.
861 2014. Symbionts commonly provide broad spectrum resistance to viruses in insects: A
862 comparative analysis of *Wolbachia* strains. PLOS Pathogens 10:e1004369.

863 Mateos, M., S. J. Castrezana, B. J. Nankivell, A. M. Estes, T. A. Markow, and N. A. Moran.
864 2006. Heritable endosymbionts of *Drosophila*. Genetics 174:363–376.

865 May, M. L. 1979. Insect thermoregulation.

866 McCutcheon, J. P., B. M. Boyd, and C. Dale. 2019. The life of an insect endosymbiont from the
867 cradle to the grave. Current Biology 29:R485–R495.

868 McCutcheon, J. P., and N. A. Moran. 2012. Extreme genome reduction in symbiotic bacteria.
869 Nature Reviews Microbiology 10:13–26.

870 McFall-Ngai, M., M. G. Hadfield, T. C. Bosch, H. V. Carey, T. Domazet-Lošo, A. E. Douglas,
871 N. Dubilier, et al. 2013. Animals in a bacterial world, a new imperative for the life sciences.
872 Proceedings of the National Academy of Sciences 110:3229–3236.

873 McInnis, D., H. Schaffer, and L. Mettler. 1982. Field dispersal and population sizes of native
874 *Drosophila* from North Carolina. The American Naturalist 119:319–330.

875 McKenzie, J. 1980. An ecological study of the alcohol dehydrogenase (Adh) polymorphism of
876 *Drosophila melanogaster*. Australian Journal of Zoology 28:709–716.

Meany, M. K., W. R. Conner, S. V. Richter, J. A. Bailey, M. Turelli, and B. S. Cooper. 2019. Loss of cytoplasmic incompatibility and minimal fecundity effects explain relatively low *Wolbachia* frequencies in *Drosophila mauritiana*. Evolution 73:1278–1295.

Newton, I. L., and D. W. Rice. 2020. The Jekyll and Hyde symbiont: could *Wolbachia* be a nutritional mutualist? Journal of Bacteriology 202.

Nikoh, N., T. Hosokawa, M. Moriyama, K. Oshima, M. Hattori, and T. Fukatsu. 2014. Evolutionary origin of insect–*Wolbachia* nutritional mutualism. Proceedings of the National Academy of Sciences 111:10257–10262.

Olsen, K., K. T. Reynolds, and A. A. Hoffmann. 2001. A field cage test of the effects of the endosymbiont *Wolbachia* on *Drosophila melanogaster*. Heredity 86:731–737.

O'Neill, S. L., R. Giordano, A. M. Colbert, T. L. Karr, and H. M. Robertson. 1992. 16S rRNA phylogenetic analysis of the bacterial endosymbionts associated with cytoplasmic incompatibility in insects. Proceedings of the National Academy of Sciences 89:2699–2702.

Osborne, S. E., Y. S. Leong, S. L. O'Neill, and K. N. Johnson. 2009. Variation in antiviral protection mediated by different *Wolbachia* strains in *Drosophila simulans*. PLOS Pathogens 5:e1000656.

Perreau, J., and N. A. Moran. 2022. Genetic innovations in animal–microbe symbioses. Nature Reviews Genetics 23:23–39.

Pietri, J. E., H. DeBruhl, and W. Sullivan. 2016. The rich somatic life of *Wolbachia*. MicrobiologyOpen 5:923–936.

Pincebourde, S., and H. A. Woods. 2012. Climate uncertainty on leaf surfaces: the biophysics of leaf microclimates and their consequences for leaf-dwelling organisms. Functional Ecology 26:844–853.

Porter, J., and W. Sullivan. 2023. The cellular lives of *Wolbachia*. Nature Reviews Microbiology 1–17.

Potter, K., G. Davidowitz, and H. A. Woods. 2009. Insect eggs protected from high temperatures by limited homeothermy of plant leaves. Journal of Experimental Biology 212:3448–3454.

Powell, J. R. 1997. Progress and prospects in evolutionary biology: the *Drosophila* model.

Radousky, Y. A., M. T. J. Hague, S. Fowler, E. Paneru, A. Codina, C. Rugamas, G. Hartzog, et al. 2023. Distinct *Wolbachia* localization patterns in oocytes of diverse host species reveal multiple strategies of maternal transmission. Genetics 224.

Rajpurohit, S., and P. S. Schmidt. 2016. Measuring thermal behavior in smaller insects: A case study in *Drosophila melanogaster* demonstrates effects of sex, geographic origin, and rearing temperature on adult behavior. Fly 10:149–161.

Rasgon, J. L., and T. W. Scott. 2004. Impact of population age structure on *Wolbachia* transgene driver efficacy: ecologically complex factors and release of genetically modified mosquitoes. Insect Biochemistry and Molecular Biology 34:707–713.

Raychoudhury, R., L. Baldo, D. C. Oliveira, and J. H. Werren. 2009. Modes of acquisition of *Wolbachia*: Horizontal transfer, hybrid introgression, and codivergence in the *Nasonia* species complex. Evolution 63:165–183.

Reynolds, K. T., and A. A. Hoffmann. 2002. Male age, host effects and the weak expression or non-expression of cytoplasmic incompatibility in *Drosophila* strains infected by maternally transmitted *Wolbachia*. Genetics Research 80:79–87.

Rigaud, T., and F. Rousset. 1996. What generates the diversity of *Wolbachia*-arthropod interactions? Biodiversity & Conservation 5:999–1013.

Roberts, S., and M. Feder. 2000. Changing fitness consequences of hsp70 copy number in transgenic *Drosophila* larvae undergoing natural thermal stress. Functional Ecology 14:353–357.

Ross, P. A., J. K. Axford, Q. Yang, K. M. Staunton, S. A. Ritchie, K. M. Richardson, and A. A. Hoffmann. 2020. Heatwaves cause fluctuations in *w*Mel *Wolbachia* densities and frequencies in *Aedes aegypti*. PLoS Neglected Tropical Diseases 14:e0007958.

Ross, P. A., S. A. Ritchie, J. K. Axford, and A. A. Hoffmann. 2019*a*. Loss of cytoplasmic incompatibility in *Wolbachia*-infected *Aedes aegypti* under field conditions. PLoS Neglected Tropical Diseases 13:e0007357.

Ross, P. A., M. Turelli, and A. A. Hoffmann. 2019*b*. Evolutionary ecology of *Wolbachia* releases for disease control. Annual Review of Genetics 53.

Ross, P. A., I. Wiwatanaratanabutr, J. K. Axford, V. L. White, N. M. Endersby-Harshman, and A. A. Hoffmann. 2017. *Wolbachia* infections in *Aedes aegypti* differ markedly in their response to cyclical heat stress. PLOS Pathogens 13:e1006006.

Rousset, F., and M. Solignac. 1995. Evolution of single and double *Wolbachia* symbioses during speciation in the *Drosophila simulans* complex. Proceedings of the National Academy of Sciences 92:6389–6393.

Russell, S. L., J. R. Castillo, and W. T. Sullivan. 2023. *Wolbachia* endosymbionts manipulate the self-renewal and differentiation of germline stem cells to reinforce fertility of their fruit fly host. PLoS Biology 21:e3002335.

Russell, S. L., L. Chappell, and W. Sullivan. 2019. A symbiont's guide to the germline. Current Topics in Developmental Biology 135:315–351.

Saudreau, M., A. Marquier, B. Adam, P. Monney, and H. Sinoquet. 2009. Experimental study of fruit temperature dynamics within apple tree crowns. Agricultural and Forest Meteorology 149:362–372.

Serbus, L. R., P. M. White, J. P. Silva, A. Rabe, L. Teixeira, R. Albertson, and W. Sullivan. 2015. The impact of host diet on *Wolbachia* titer in *Drosophila*. PLoS pathogens 11:e1004777.

Shropshire, J. D., W. R. Conner, D. Vanderpool, A. A. Hoffmann, M. Turelli, and B. S. Cooper. 2024. Rapid host switching of *Wolbachia* and even more rapid turnover of their phages and incompatibility-causing loci. bioRxiv.

Shropshire, J. D., E. Hamant, and B. S. Cooper. 2021. Male age and *Wolbachia* dynamics: investigating how fast and why bacterial densities and cytoplasmic incompatibility strengths vary. mBio 12:e02998-21.

Shropshire, J. D., B. Leigh, and S. R. Bordenstein. 2020. Symbiont-mediated cytoplasmic incompatibility: what have we learned in 50 years? Elife 9:e61989.

Teixeira, L., Á. Ferreira, and M. Ashburner. 2008. The bacterial symbiont *Wolbachia* induces resistance to RNA viral infections in *Drosophila melanogaster*. PLoS Biology 6:e1000002.

Turelli, M. 2010. Cytoplasmic incompatibility in populations with overlapping generations. Evolution 64:232–241.

Turelli, M., and N. H. Barton. 2022. Why did the *Wolbachia* transinfection cross the road? drift, deterministic dynamics, and disease control. Evolution Letters 6:92–105.

Turelli, M., B. S. Cooper, K. M. Richardson, P. S. Ginsberg, B. Peckenpaugh, C. X. Antelope, K. J. Kim, et al. 2018. Rapid global spread of *w*Ri-like *Wolbachia* across multiple *Drosophila*. Current Biology 28:963-971.e8.

Turelli, M., and A. A. Hoffmann. 1991. Rapid spread of an inherited incompatibility factor in California *Drosophila*. Nature 353:440–442.

Turelli, M., and A. A. Hoffmann. 1995. Cytoplasmic incompatibility in *Drosophila simulans*: dynamics and parameter estimates from natural populations. Genetics 140:1319–1338.

Turelli, M., A. Katznelson, and P. S. Ginsberg. 2022. Why *Wolbachia*-induced cytoplasmic incompatibility is so common. Proceedings of the National Academy of Sciences 119:e2211637119.

Ulrich, J. N., J. C. Beier, G. J. Devine, and L. E. Hugo. 2016. Heat sensitivity of *w*Mel *Wolbachia* during *Aedes aegypti* development. PLoS Neglected Tropical Diseases 10:e0004873.

Unckless, R. L., L. M. Boelio, J. K. Herren, and J. Jaenike. 2009. Wolbachia as populations within individual insects: causes and consequences of density variation in natural populations. Proceedings of the Royal Society B: Biological Sciences 276:2805–2811.

Vancaester, E., and M. Blaxter. 2023. Phylogenomic analysis of *Wolbachia* genomes from the Darwin Tree of Life biodiversity genomics project. PLoS Biology 21:e3001972.

Versace, E., V. Nolte, R. V. Pandey, R. Tobler, and C. Schlötterer. 2014. Experimental evolution reveals habitat-specific fitness dynamics among *Wolbachia* clades in *Drosophila melanogaster*. Molecular Ecology 23:802–814.

Wade, M. J. 2007. The co-evolutionary genetics of ecological communities. Nature Reviews Genetics 8:185–195.

Weeks, A. R., M. Turelli, W. R. Harcombe, K. T. Reynolds, and A. A. Hoffmann. 2007. From parasite to mutualist: Rapid evolution of *Wolbachia* in natural populations of *Drosophila*. PLoS Biology 5:e114.

Weinert, L. A., E. V. Araujo-Jnr, M. Z. Ahmed, and J. J. Welch. 2015. The incidence of bacterial endosymbionts in terrestrial arthropods. Proceedings of the Royal Society B: Biological Sciences 282:20150249.

Wood, S. N. 2017. Generalized additive models: an introduction with R. Chapman and Hall/CRC.

Woods, H. A., M. E. Dillon, and S. Pincebourde. 2015. The roles of microclimatic diversity and of behavior in mediating the responses of ectotherms to climate change. Journal of Thermal Biology 54:86–97.

995 Zug, R., and P. Hammerstein. 2012. Still a host of hosts for *Wolbachia*: Analysis of recent data
996 suggests that 40% of terrestrial arthropod species are infected. PLoS One 7:e38544.
997

998 **TABLES**

999 **Table 1.** Regression analysis of the effects of model parameters on the standard deviation of

1000 *Wolbachia* frequencies (p_{SD}).

		Coefficient	t value	*P* value
	Host population size	-4.14×10^{-7}	-1.13×10^{2}	< 0.001
Imperfect maternal transmission (μ)	**μ value ($0.001 \leq \mu \leq 0.5$)**	8.51	4.03×10^{2}	< 0.001
	Low transmitters	1.12	2.88×10^{2}	< 0.001
	μ value * low transmitters	-4.42	-1.39×10^{2}	< 0.001
Host fitness effects (F)	**F value ($1 \leq F \leq 1.5$)**	-2.04	-1.68×10^{2}	< 0.001
	Fluctuating F ($CV = 0.01$)	4.23×10^{-1}	1.01×10^{2}	< 0.001
	Fluctuating F ($CV = 0.1$)	1.78	4.49×10^{2}	< 0.001
Cytoplasmic incompatibility (s_h)	**Weak CI ($s_h = 0.1$)**	-9.85×10^{-2}	-3.20×10^{1}	< 0.001
	Strong CI ($s_h = 0.45$)	-7.83×10^{-1}	-2.17×10^{2}	< 0.001

1001

1002 **Table 2.** Regression analysis of the effects of model parameters on mean *Wolbachia* frequencies

1003 ($\bar{p}$).

		Coefficient	t value	*P* value
	Host population size	-1.58×10^{-8}	-6.09	< 0.001
Imperfect maternal transmission (μ)	**μ value ($0.001 \leq \mu \leq 0.5$)**	-2.24×10^{1}	-1.02×10^{3}	< 0.001
	Low transmitters	-2.43	-7.33×10^{2}	< 0.001
	μ value * low transmitters	8.26	2.76×10^{2}	< 0.001
Host fitness effects (F)	**F value ($1 \leq F \leq 1.5$)**	3.77	4.01×10^{2}	< 0.001
	Fluctuating F ($CV = 0.01$)	1.30×10^{-4}	4.93×10^{-2}	9.61×10^{-1}
	Fluctuating F ($CV = 0.1$)	9.68×10^{-3}	3.62	< 0.001
Cytoplasmic incompatibility (s_h)	**Weak CI ($s_h = 0.1$)**	4.27×10^{-1}	1.63×10^{2}	< 0.001
	Strong CI ($s_h = 0.45$)	1.92	6.82×10^{2}	< 0.001

1004

1005

1006 **FIGURES**

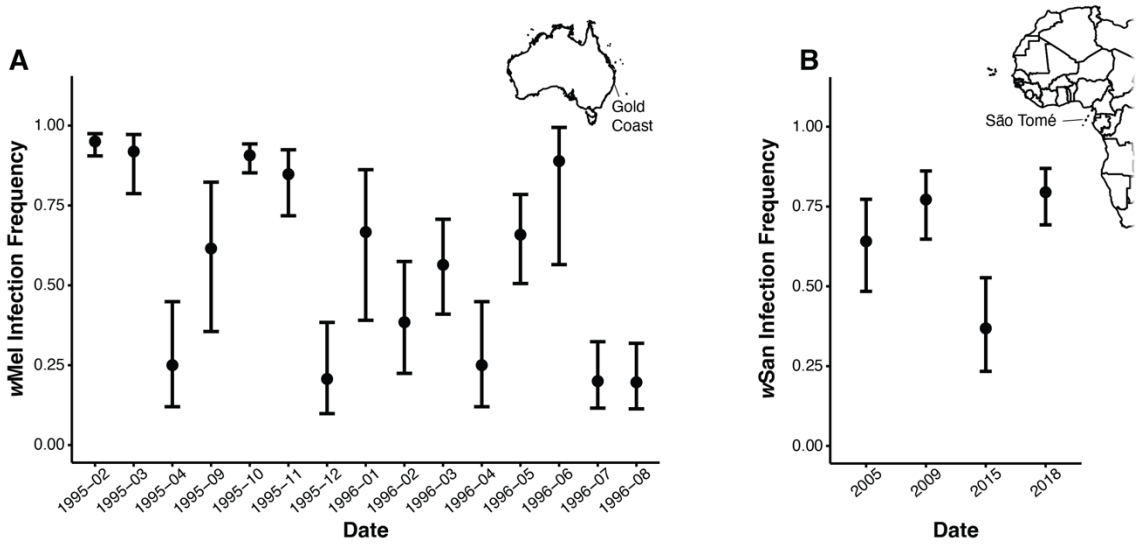

1007

1008 **Figure 1.** Temporal fluctuations of *Wolbachia* frequencies for **(A)** *w*Mel in *D. melanogaster* and

1009 **(B)** *w*San in *D. santomea*. Error bars represent 95% binomial confidence intervals. **(A)** *w*Mel

1010 frequencies in *D. melanogaster* at Gold Coast in subtropical eastern Australia from the winter of

1011 1995 to the summer of 1996. Data recreated from Hoffmann et al. (1998). The authors reported

1012 no obvious seasonal effect on *w*Mel frequencies. **(B)** *w*San frequencies in *D. santomea* in the

1013 high-altitude mist forests on the volcanic island of São Tomé estimated from 2005 to 2018. Data

1014 recreated from Hague et al. (2020*b*). *w*Yak frequencies in *D. yakuba* also fluctuate temporally on

1015 São Tomé; however, this variation is complicated by altitudinal variation in *Wolbachia*

1016 frequencies and transmission rates (Hague et al. 2020*b*).

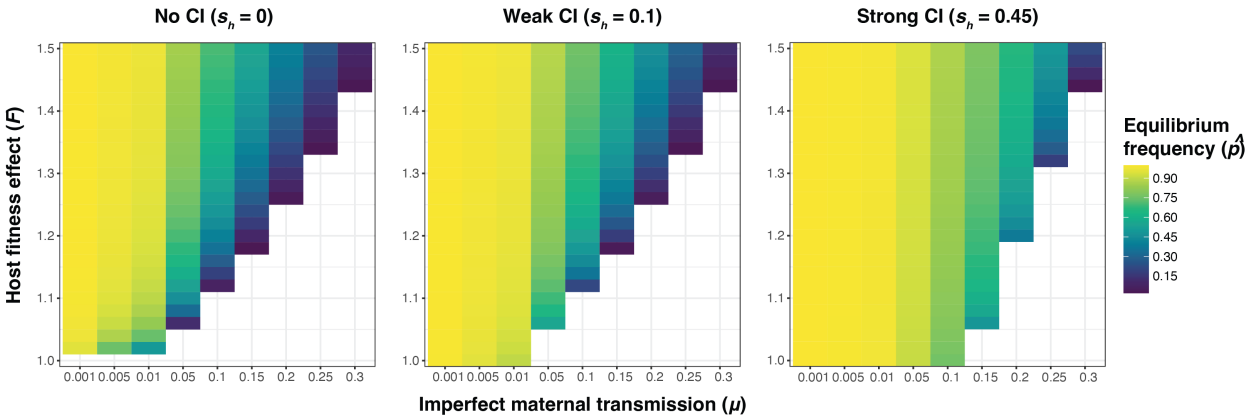

Figure 2. Equilibrium *Wolbachia* frequencies ($\hat{p}$) approximated by a discrete generation deterministic model incorporating imperfect maternal transmission (μ), *Wolbachia* effects on host fitness (F), and cytoplasmic incompatibility (s_h). Equilibrium frequencies are shown across a range of biologically plausible parameter values for no, weak, and strong CI.

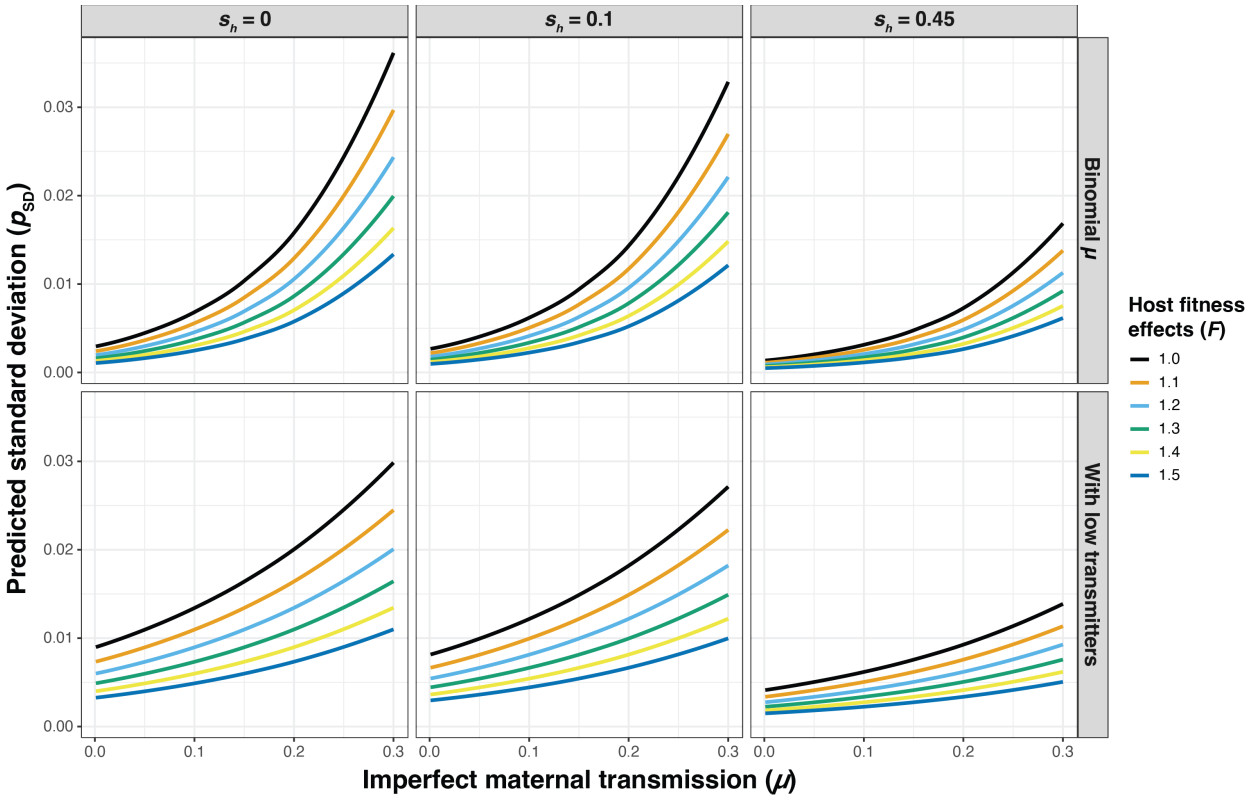

1022

1023 **Figure 3.** Predicted standard deviation (p_{SD}) values of *Wolbachia* frequencies over time from the

1024 regression analysis as a function of imperfect maternal transmission (μ) and conditioned by the

1025 presence/absence of low transmitters, strength of host fitness effects (F), and cytoplasmic

1026 incompatibility (s_h). Note that prediction lines average the effects of host population size (N) and

1027 fixed/fluctuating host effects (CV = 0.01 and 0.1).

1028

1029

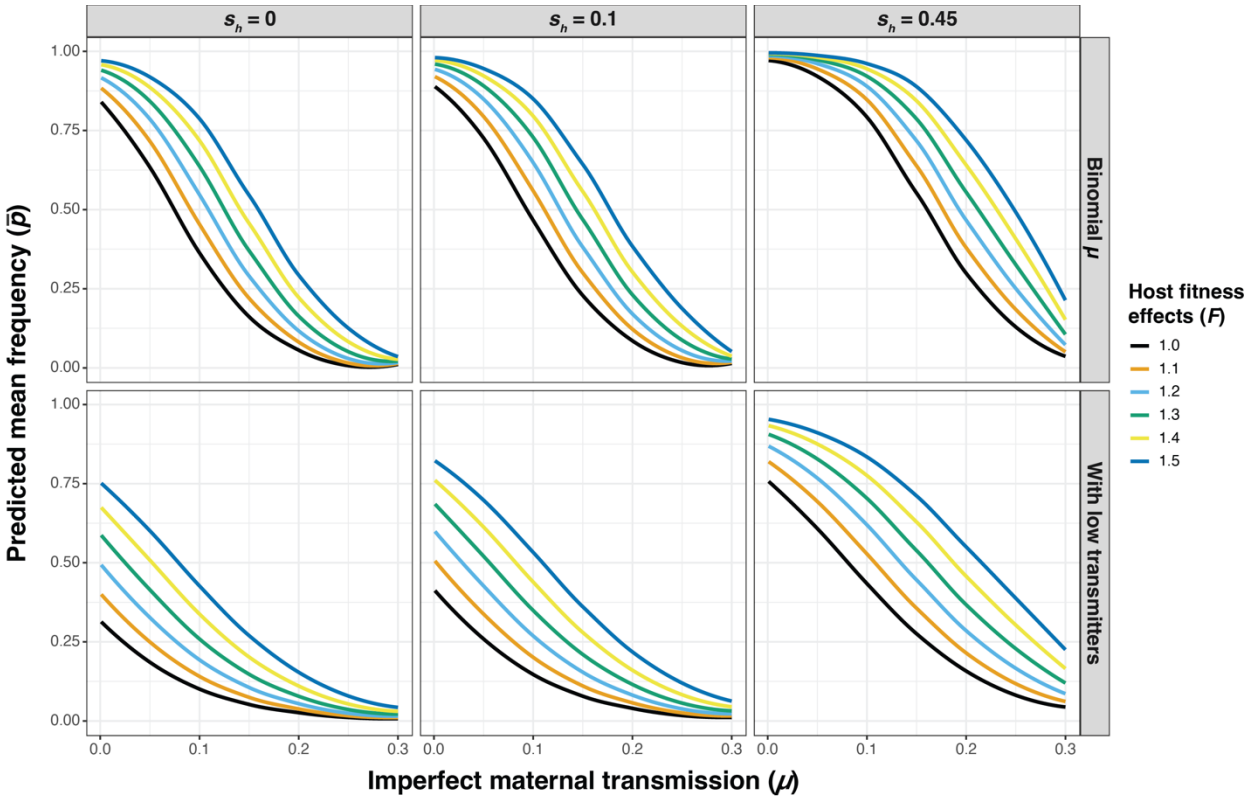

Figure 4. Predicted mean *Wolbachia* frequency ($\bar{p}$) values from the regression analysis as a function of imperfect maternal transmission (μ) and conditioned by the presence/absence of low transmitters, strength of host fitness effects (F), and cytoplasmic incompatibility (s_h). Note that prediction lines average the effects of host population size (N) and fixed/fluctuating host effects (CV = 0.01 and 0.1).

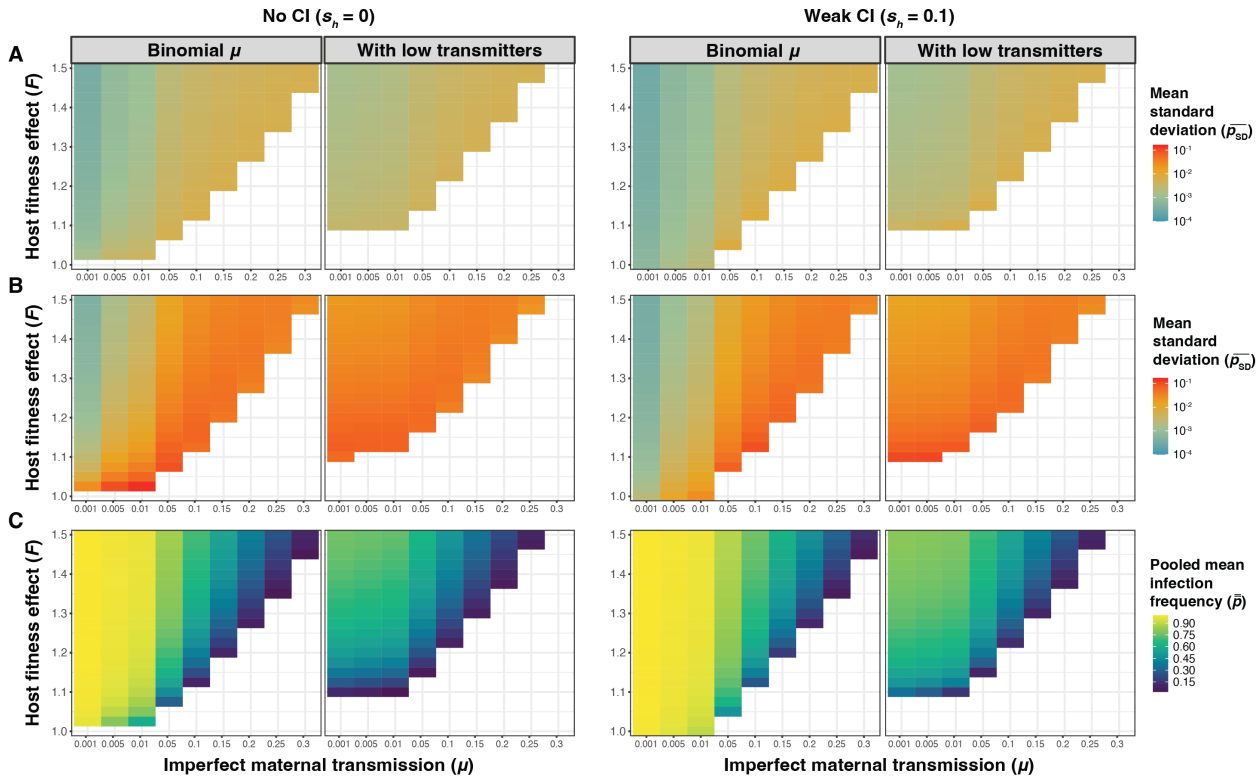

Figure 5. Summary of results from simulations exploring the contributions of μ, F, and s_h to standard deviations (p_{SD}) and mean *Wolbachia* frequencies ($\bar{p}$) with a finite host population size of $N = 10^4$. **(A)** Each cell represents the mean standard deviation ($\overline{p_{SD}}$) of *Wolbachia* frequencies from 25 simulations with a given μ value and a fixed F value. Note that $\overline{p_{SD}}$ values are plotted on a log scale. **(B)** Each cell represents $\overline{p_{SD}}$ from 25 simulations with a given μ value and a strongly fluctuating F value ($CV = 0.1$). **(C)** Each cell represents the pooled mean of mean *Wolbachia* frequencies ($\bar{\bar{p}}$) from a set of 25 simulations with a given μ value and a fixed F value. Similar data are not shown for the simulations with fluctuating F values, because fluctuating host effects had only a small effect on $\bar{p}$. Results for strong CI (considered implausible for *w*Mel and *w*San) are shown in Figure S3.

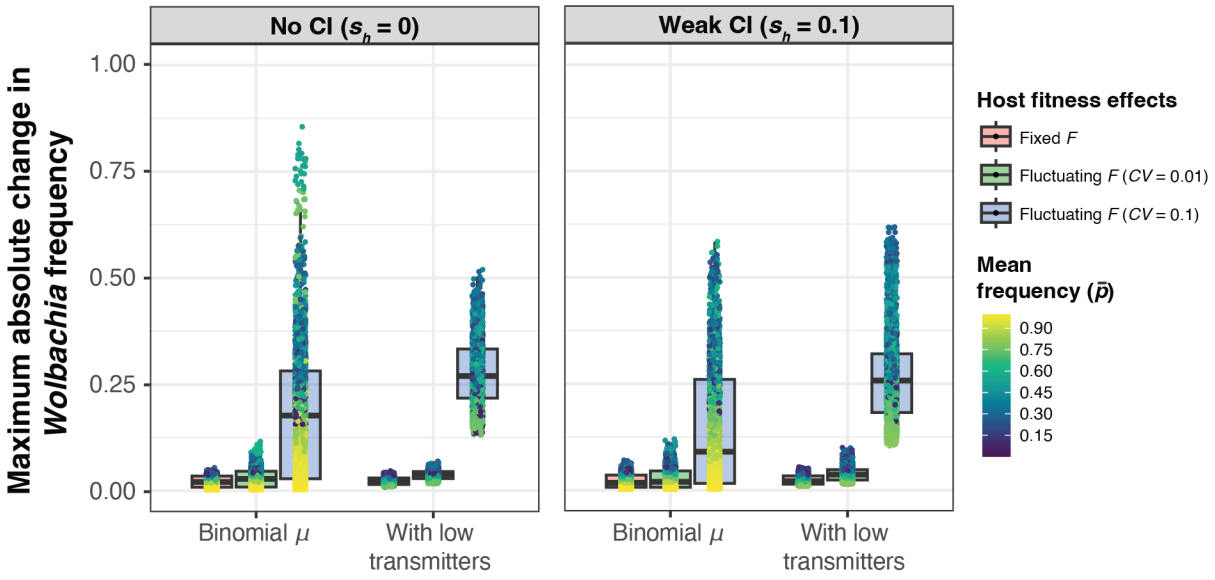

Figure 6. Results from individual simulations exploring the contributions of μ, F, and s_h to the absolute difference between maximum and minimum *Wolbachia* frequencies (p_{max} - p_{min}) observed over 10,000 host generations with a finite population size of $N = 10^4$. Individual points represent the maximum absolute change in *Wolbachia* frequencies observed in a given simulation with various combinations of μ ($0.001 \leq \mu \leq 0.5$) and F ($1 \leq F \leq 1.5$). Datasets are further separated based on whether low transmitters and fluctuating host effects (CV = 0.01 or 0.1) are present. Individual points are color-coded to indicate each simulation's mean *Wolbachia* frequency ($\bar{p}$). The full set of results are shown in Figure S4. The first 500 generations were removed from each simulation before calculating p_{max} - p_{min}.